Noname manuscript No.
(will be inserted by the editor)

EUREC^{4}A: a field campaign to elucidate the couplings between clouds, convection and circulation

Sandrine Bony · Bjorn Stevens · Felix Ament · Susanne Crewell · Julien Delanoë · David Farrell · Cyrille Flamant · Silke Gross · Lutz Hirsch · Bernhard Mayer · Louise Nuijens · James H. Ruppert Jr. · Irina Sandu · Pier Siebesma · Sabrina Speich · Frédéric Szczap · Raphaela Vogel · Manfred Wendisch · Martin Wirth

January 14, 2017

S. Bony, S. Speich
LMD/IPSL, CNRS, UPMC Univ Paris 06, Ecole Normale Supérieure, 4 Place Jussieu, 75252 Paris cedex 05, France E-mail: bony@lmd.jussieu.fr

B. Stevens, L. Hirsch, J. H. Ruppert Jr., R. Vogel
Max Planck Institute for Meteorology, Bundesstr. 53, D-20146 Hamburg, Germany

F. Ament
University of Hamburg, Bundesstrasse 55, 20146 Hamburg, Germany

S. Crewell,
University of Cologne, Albertus-Magnus-Platz, D-50923 Cologne, Germany

J. Delanoë, C. Flamant
LATMOS/IPSL, UVSQ, UPMC, 11 Boulevard D'Alembert, 78280 Guyancourt, France

D. Farrell
Caribbean Institute for Meteorology and Hydrology, P.O. Box 130, Bridgetown, Barbados

S. Gross, M. Wirth
German Aerospace Center, Múnchener Str. 20, 82234 Oberpfaffenhofen-Wessling, Germany

B. Mayer
Meteorological Institute Munich, Theresienstrasse 37, 80333 Muenchen, Germany

L. Nuijens, A. P. Siebesma
Delft University of Technology, P.O. Box 5048, 2600 GA Delft, The Netherlands

I. Sandu
ECMWF, Shinfield Park, RG2 9AX Reading, UK

F. Szczap
Laboratoire de Météorologie Physique, UMR6016, CNRS, Aubière, France

M. Wendisch
University of Leipzig, Stephanstr. 3, 04103 Leipzig, Germany

Abstract Trade-wind cumulus clouds constitute the most prominent cloud type on Earth, and their response to changing environmental conditions is critical for the fate of climate. Research over the last decade has pointed out the importance of the interplay between clouds, convection and circulation in controling this response. Unfortunately, numerical models represent this interplay in diverse ways, which translates into different responses of trade-cumulus clouds to climate perturbations. Climate models predict that the cloud-base cloud fraction is very sensitive to changes in environmental conditions, while process models suggest that it is very resilient to such changes. To understand and solve this contradiction, we propose to organize a field campaign aimed at quantifying the macrophysical properties of trade-cumulus clouds (e.g. cloud fraction and water content) as a function of the large-scale environment. Beyond a better understanding of clouds-circulation coupling processes, the campaign will provide a reference dataset that may be used as a benchmark for advancing the modelling and the satellite remote sensing of clouds and circulation. It will also be an opportunity for complementary science investigations such as studies of the role of ocean mesoscale eddies in air-sea interactions and convective organization.

Keywords Trade-cumulus clouds · Shallow convection · Cloud feedback · Atmospheric circulation · Field campaign

1 Introduction

In a climate increasingly perturbed by human activities, it is urgent to anticipate the pace of global warming and of regional changes in rainfall and extreme events that will occur over the next decades. This necessitates a deeper understanding of the interplay between clouds, atmospheric circulations and climate sensitivity (Bony et al, 2015), as recognized by the World Climate Research Programme which has considered this imperative as one of its Grand Science Challenges for the next decade.

From all the clouds that populate the Earth's atmosphere, trade-cumulus clouds count amongst the most fascinating expressions of the interplay between clouds and circulations. These broken shallow clouds form within the lowest kilometers of the atmosphere, influenced at their base by small-scale turbulent motions of the warm, moist surface layer and at their top by the large-scale sinking motions of the dry, quiescent free troposphere. If many of these clouds do not rise by more than a few hundred meters above their base, some reach higher levels and detrain and help sustain the trade-wind temperature-inversion layer higher up. Trade-cumuli warm the layer in which they form through condensation, but cool the subcloud layer and the trade inversion through the evaporation of detrained droplets and falling raindrops. In addition, the emission of infrared radiation to space produces an efficent cooling of the lower atmosphere in which clouds form. This cooling generates shallow mesoscale circulations which, depending on local conditions and remote convective activity, can organize either randomly or into streets, arcs or

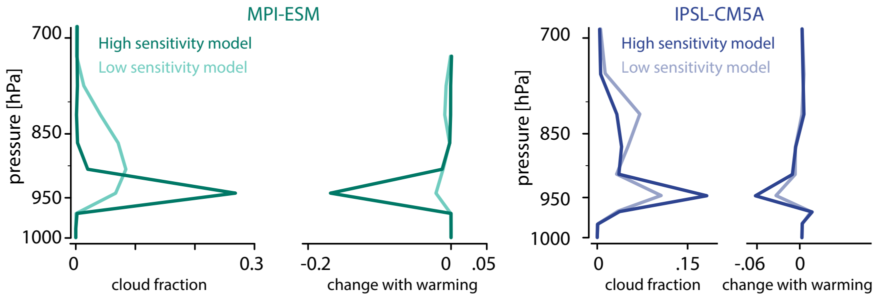

Fig. 1: Vertical profiles of the low-cloud fraction, and its response to global warming, predicted by two general circulation models (MPI and IPSL) in the trades. For each model, results are shown for two versions differing only by their representation of lower-tropospheric mixing (after Stevens et al, 2016; Vial et al, 2016).

circles of cloud clusters. In certain conditions, these mesoscale circulations can also trigger remotely the aggregation of deep convection (Muller and Held, 2012).

This coupling between shallow clouds and circulation greatly matters for climate sensitivity. Trade-cumulus clouds are so ubiquitous over tropical oceans that their radiative properties substantially influence the Earth's radiation budget. Their response to global warming is thus critical for global-mean cloud feedbacks, and as a matter of fact, it is their differing response to warming that explains most of the spread of climate sensitivity across climate models (Bony et al, 2004; Bony and Dufresne, 2005; Webb et al, 2006; Medeiros et al, 2008; Vial et al, 2013; Boucher et al, 2013; Medeiros et al, 2015). Model diversity in the strength of the vertical mixing of water vapour within the first few kilometres above the ocean surface (in association with both convective and large-scale circulations) is thought to explain half of the variance in climate sensitivity estimates (Sherwood et al, 2014): lower-tropospheric mixing dehydrates the cloud layer near its base at an increasing rate as the climate warms, which scales with the mixing strength in the current climate (Sherwood et al, 2014; Gettelman et al, 2012; Tomassini et al, 2015; Brient et al, 2016; Vial et al, 2016), Figure 1). There is increasing evidence that the diversity of the modeled response to warming reflects model diversity in how this coupling between convective mixing, surface turbulent fluxes and low-cloud radiative effects is represented in regimes of large-scale subsidence, and that it can be partly related to the numerical representation (or parameterization) of convection (Webb et al, 2015; Vial et al, 2016). However, so far it has not been possible to constrain this coupling observationally due to a lack of appropriate measurements.

In large-eddy simulation (LES) models (that do not use any parameterization of clouds and convection) and in in-situ observations, on the contrary, the trade-cumulus cloud fraction appears to be much more resilient to changes in environmental conditions than in climate models, both in the current (Nuijens et al, 2014, 2015) and projected climate (Rieck et al, 2012; Bretherton, 2015). Interpreting these results remains difficult. For the observations, in the past it has not been possible to link cloud amount to the large-scale circulation in which the clouds form. Cloud amount simulated by LES models, though often resilient to changes in thermodynamic conditions, is known to be sensitive to various aspects of the simulation, including resolution, microphysics, numerics and domain size (Matheou et al, 2011; Seifert and Heus, 2013; Vogel et al, 2016). Theoretically, the apparent resilience of cloud-base cloud amount has been interpreted as the consequence of a "cumulus-valve mechanism" that regulates the area covered by cumulus updrafts at cloud base (Albrecht et al, 1979; Neggers et al, 2006; Stevens, 2006; Nuijens et al, 2015). However, this idea has not been verified by observations. Moreover, recent studies running LES simulations over large domains question this idea of cloud-base resilience, as they show that changes in the mesoscale organization of shallow cumulus clouds can significantly impact the cloud fraction (Seifert and Heus, 2013; Vogel et al, 2016). It is thus paramount to assess the ability of LES models to predict the cloud cover and its dependence on the organization of convection and on environmental conditions.

The discussion above illustrates how the science has matured to the point where it is now possible to identify a few key hypotheses or questions that, if tested with targeted observations and a hierarchy of numerical experiments, would enable a step improvement in our understanding of the interplay between clouds, convection and circulation, and their role in climate change: How strong is the convective mixing in regimes of shallow cumulus? How much does it couple to surface turbulent fluxes and cloud-radiative effects? How resilient or sensitive is the trade-cumulus cloud cover to variations in the strength of convective mixing and large-scale circulations? Can the valve mechanism be tested with observations? How much of the surface source of enthalphy is encountered by convective downdrafts vs clear-air turbulent entrainment vs radiative cooling? How much does the spatial organization of shallow convection matter for these different aspects?

Improved observations are also necessary to help advance space-based remote sensing. The trades are characterized by a strongly layered vertical structure, and by warm, small, thin broken clouds. Current satellite observations are inadequate to detect sharp vertical gradients of water vapor (Chazette et al, 2014; Asrar et al, 2015, Stevens et al., this volume), and the detection of shallow clouds from space remains difficult. Biases in cloud detection leads to significant discrepancies among the various satellite estimates of the trade-cumulus cloud fraction (Stubenrauch et al, 2013) and is detrimental to the quality of other satellite retrievals such as those of the cloud water path (Horváth and Gentemann, 2007) or precipitation. In these conditions, in-situ observations are not only critical to investigate the physics of trade-cumulus clouds, but also to test – and eventually improve – the instruments and algorithms of remote sensing that are used to observe the Earth's atmosphere and surface from space.

Past field campaigns in regions of shallow cumulus such as the *Atlantic Expedition* in Sept-Oct 1965 (Augstein et al, 1973), the *Atlantic Tradewind EXperiment* in Feb 1969 (ATEX, Augstein et al, 1974), the *Barbados Oceanographic and Meteorological Experiment* during May-Jul 1969 (BOMEX, Holland, 1970) or the *Puerto-Rico Experiment* in Dec 1972 (LeMone and Pennell, 1976), did focus on the environment of clouds, on vertical transports of water, heat and momentum in the trade-wind boundary layer, and provided the first measurements of large-scale vertical motions in the atmosphere. However, the microphysical and macrophysical properties of the shallow cumuli were not characterized. Because these campaigns took place at the dawn of the satellite era, no observations from space could help fill the gap. In June 1992, the *Atlantic Stratocumulus Transition Experiment* (ASTEX, Albrecht et al, 1995) was conducted off North Africa, in the area of Azores and Madeira Islands, to address issues related to the stratocumulus to trade-cumulus transition and cloud-mode selection. Satellites and upper-level aircraft provided a description of large-scale cloud features, and instrumented aircraft flying in the boundary layer and surface-based remote sensing systems provided a description of the mean, turbulence, and mesoscale variability in microphysical properties of boundary layer clouds. Large-scale divergence in the boundary-layer was inferred from an array of three rawinsondes (Ciesielski et al, 1999). In 2005, the *Rain in shallow cumulus over the ocean* experiment (RICO, Rauber et al, 2007) that took place off the Caribbean islands of Antigua and Barbuda did focus on cloud microphysical properties, but not on the interplay between cloud macrophysical properties (e.g. the low-level cloud fraction) and their environment. The establishement of the Barbados Cloud Observatory (BCO) in 2010, and the two *Next-Generation Aircraft Remote Sensing for Validation Studies* airborne field campaigns (NARVAL and NARVAL2) held in December 2013 and August 2016 demonstrate the power of advanced remote sensing instrumentation to characterize clouds and their environment, and to evaluate satellite retrievals (Stevens et al, 2016). However, the simultaneous observation of clouds, convection, large-scale dynamics and thermodynamics, surface properties and atmospheric radiation is still lacking. During NARVAL2, however, new approaches were tested for bridging the gap between measurements of cloud macro-structure and the large-scale environment.

A new field campaign, EUREC^{4}A (*Elucidating the role of clouds-circulation coupling in climate*), has been designed to take advantage of and extend these advances. It will take place in the winter trades of the North Atlantic, near Barbados, in early 2020, and will have two primary objectives:

1. To quantify macrophysical properties of trade-cumulus clouds as a function of the large-scale environment, and

2. To provide a reference data set that may be used as a benchmark for the modelling and the satellite observation of clouds and circulation.

To address these objectives EUREC^{4}A will provide, for the first time, simultaneous measurement of cloud macrophysical properties (cloud fraction, vertical extent and cloud-size distributions), cloud optical properties, convective activity (cloud-base mass flux, mesoscale organization) and the large-scale environment in which clouds and convection are embedded (large-scale vertical motion, thermodynamic stratification, surface properties, turbulent and radiative sources or sinks of energy).

In section 2, we present an overview of the experimental strategy for the EUREC^{4}A field campaign. In section 3, we discuss the premises which are at the basis of this strategy, namely the possibility to measure cloud profiles, (especially cloud amount at cloud base), convective mass flux and large-scale vertical velocity, as only this can connect the macrophysical properties of clouds to the environment. Then we discuss how the results from the campaign could be used to build a reference dataset for evaluating process and climate models, and for assessing retrievals from space-borne observations (section 4). Beyond the study of clouds-circulation interactions, EUREC^{4}A will be an opportunity for complementary scientific investigations. Several such examples are presented in section 5.2. We end up (section 6) by encouraging the nucleation of more international efforts around the campaign.

2 Overview of the EUREC^{4}A experimental strategy

The core objective of the EUREC^{4}A field campaign is to elucidate how the macrophysical properties of trade-cumulus clouds depend on the dynamic and thermodynamic properties of the environment in which clouds form. More specifically, EUREC^{4}A aims to answer the following questions:

- What controls the convective mass flux, mesoscale organization and depth of shallow-cumulus clouds?
- How does the trade-cumulus cloud fraction vary with turbulence, convective mixing and large-scale circulations, and what impact does this variation have on the atmospheric radiation field?

The EUREC^{4}A field campaign will take place in the lower Atlantic trades, over the ocean east of Barbados (13 °N, 57 °W) during winter (20 January - 20 February 2020). Several reasons motivate the choice of this specific location. First, shallow cumulus clouds are prominent in this area, especially during winter (Norris, 1998; Nuijens et al, 2014). Second, the cloudiness in the vicinity of Barbados is representative of clouds across the whole trade-wind regions of the tropical ocean, both in models and in observations (Medeiros and Nuijens, 2016). Third, it is close to the extensively instrumented Barbados Cloud Observatory which has been monitoring clouds continuously since 2010 (Stevens et al, 2016). Finally, it benefits from the legacy of the field campaigns previously organized in the area (ATEX, ASTEX, BOMEX, RICO, NARVAL, NARVAL2). The collective expertise and scientific insights developed by the community participating in these field studies will be invaluable to ensure the success of the EUREC^{4}A campaign.

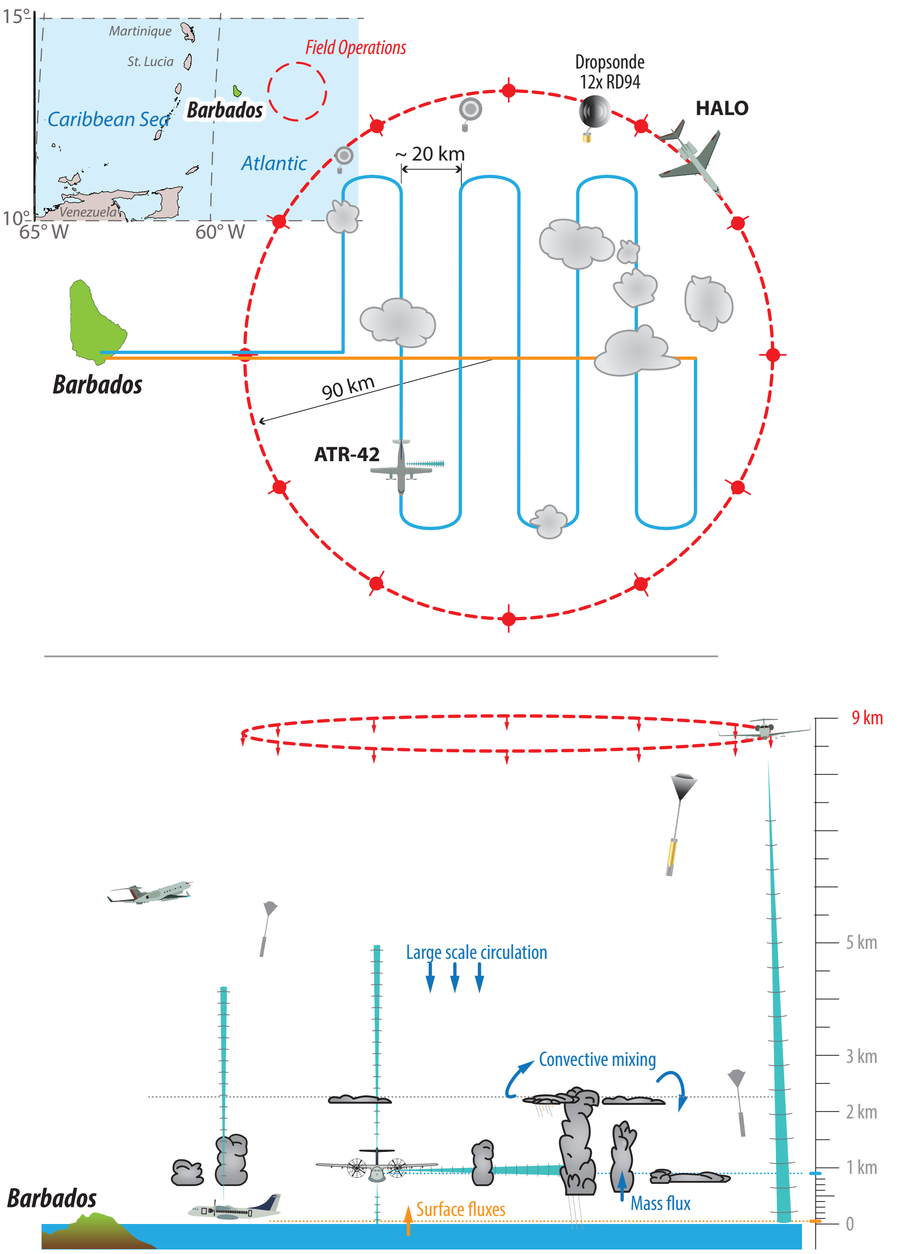

Fig. 2: Envisioned flight strategy for the EUREC^{4}A core measurements.

2.1 Aircraft measurements

The primary motivation for EUREC^{4}A is the need to characterize simultaneously the shallow cumulus cloud field and the dynamic and thermodynamic environment in which it forms. For this purpose, the core of the EUREC^{4}A field campaign will be the deployment of two research aircraft (Figure 2): The French ATR-42 operated by the Service des Avions Français Instrumentés pour la Recherche en Environnement (SAFIRE), which has the ability to fly in the lower-troposphere with a payload of up to two tons and will be equipped with both remote sensing instrumentation and a suite of in situ sensors, and the German HALO (High Altitude and LOng range) operated by the Deutsches Zentrum für Luft- and Raumfahrt (DLR), which has a payload of up to three tons, a range of up to 8000 km and a ceiling of up to 15 km, an advanced instrumentation and the ability to launch dropsondes (see for instance Wendisch et al, 2016). In addition to these aircraft, we will use the Barbados Cloud Observatory (BCO) plus several research vessels deployed in the area and equipped with rawinsondes and additional remote sensing instruments to form a large-scale sounding array (LSA, section 2.2) and to provide additional surface, atmospheric and ocean measurements.

HALO will fly large circle patterns (45-50 min, corresponding to a circumference of about 500 km) at 9 km altitude (FL300), and will launch a dense array of dropsondes along the circles. The dropsondes will characterize the vertical thermodynamic structure of the trade-wind atmosphere and will allow to infer the vertical profile of large-scale divergence over the area (section 3.1). The advanced remote sensing instrumentation on board the aircraft will characterize the cloud field and its environment (water vapor, hydrometeors, cloud particle phase, cloud vertical structure, cloud reflectivity, etc).

Simultaneously, the ATR-42 will characterize the shallow cumulus cloud field and boundary-layer properties within the area through a series of low-level legs, flown either just above cloud base ($\sim$1 km) or near the sea surface. Sideways-staring lidar and radar instruments will measure the cloud fraction near cloud base (section 3.2). Intermittent upward-pointing high spectral resolution (HSR) backscatter lidar observations will be used to assess the boundary-layer depth and measure the vertical velocity in the aerosol-laden lower troposphere above the aircraft. Other instruments on board the aircraft will characterize cloud microphysical properties, the tri-dimensional wind field at the altitude of the aircraft, and the turbulence within the subcloud-layer (Appendix A). Dedicated legs will also be performed near the surface, to measure surface turbulent fluxes, near-surface temperature and sea surface temperature.

The advanced instrumentation on board both aircraft, including multi-wavelength backscatter and water-vapor lidars, multi-frequency doppler radars and radiometers operating across a wide array of frequencies, will provide a detailed characterization of the vertical distribution of water vapor, clouds and aerosol particles, and of vertical velocities within clouds (Appendix A). Measurements of radiative fluxes at different altitudes, as well as radiative transfer calculations using observed atmospheric and cloud properties, will allow to infer vertical profiles of radiative solar heating and terrestrial cooling rates.

The characterization of subcloud-layer properties and of the difference between the subcloud layer and the air just above it, combined with estimates of surface turbulent fluxes, radiative cooling and large-scale mass divergence, will allow to close the mass and moist static energy budgets of the subcloud layer. The analysis of the mass budget will make it possible to estimate the cumulus mass flux at cloud base (section 3.3). The moist static energy budget will allow to verify the consistency among the different measurements.

To maximize the chance of sampling a large diversity of environmental conditions and mesoscale organizations, the campaign will consist of about 90 hours of research flight (for each aircraft) over four weeks for operations out of Grantley Adams International Airport on Barbados. It is envisioned to have ten HALO research flights from Barbados, each with a duration of 9 hrs bracketing two 4-hr flights of the ATR-42 (with a refueling in between).

2.2 Large-scale sounding array and ship-based observations

In addition to the aircraft missions that will characterize clouds and their surrounding environment up to scales of O(100 km), a large-scale sounding array will be established to diagnose thermodynamic properties and air motions on a scale of O(1000 km) and over a longer, uninterrupted time period. It will provide context for the airborne measurements relative to the diurnal cycle, transient disturbances (such as easterly waves), intraseasonal variability, and other modes of large-scale variability.

The LSA will be comprised of three to five stations (Figure 3): the Barbados Cloud Observatory (BCO, Stevens et al, 2016) and a network of research vessels (RVs) stationed in the trades upstream of Barbados (near 50 °W). Applications for ship measurement time from Germany (*Meteor* and *Maria S. Merian*), The Netherlands (*Pelagia*) and the United States are pending. Rawinsondes will be launched from each station to collect simultaneous profiles of humidity, temperature, pressure and (thanks to GPS measurements) horizontal winds from the surface through the lower stratosphere. Large-scale divergence and vertical motion will then be diagnosed from these synchronized soundings. The accuracy of this divergence calculation increases with the number of stations; hence, earnest efforts to procure additional RVs are underway. The LSA will operate over a twelve-week extended observing period (EOP), with an equal buffer of approximately four weeks prior to commencement and following completion of the aircraft missions. This three-month EOP will establish context for the aircraft missions relative to the seasonal march of the ITCZ and the evolving strength of overturning within the Hadley cell. Soundings will be launched with a minimum frequency of 6 day^{-1} during the EOP in order to adequately sample the diurnal and semi-diurnal cycles, along with other sub-daily variability. During the four-week period of aircraft mis-

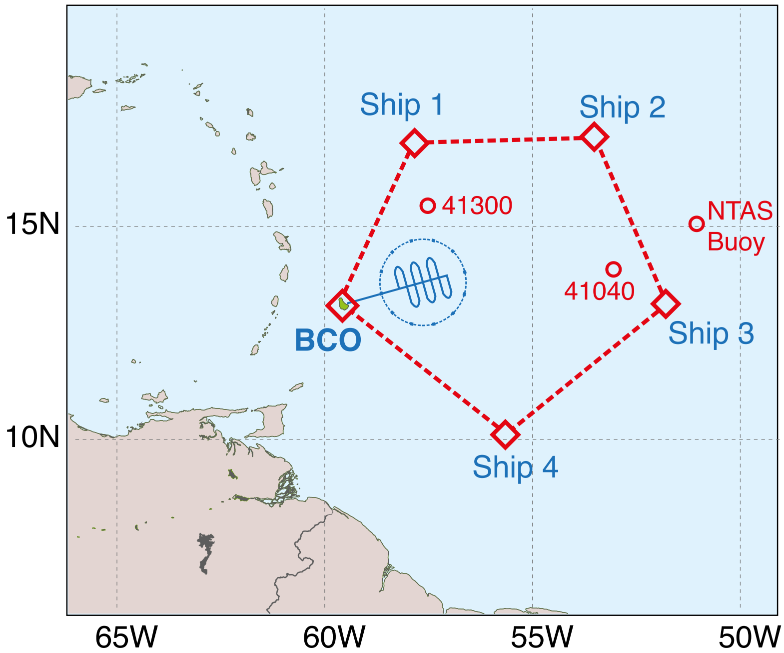

Fig. 3: Large-scale sounding array (LSA) envisioned for EUREC^{4}A, comprised by the Barbados Cloud Observatory (BCO) and approximately four research vessels (R/Vs). The R/Vs may include the Meteor and Merian (Germany), the Pelagia (the Netherlands), and a possible U.S. ship (LSA stations are indicated by squares, and buoy stations by open circles). Rawinsondes will be launched simultaneously at a rate of 6 day^{-1} from each LSA station. Radar and surface flux measurements may also be conducted from some of the ship sites.

sions (the intensive observing period; IOP), the sounding launch frequency will be increased to 12 day^{-1} to augment the accuracy of diurnal sampling, and to ensure representativeness of the LSA measurements for the aircraft missions. Mock-arrangements of the sounding array will be explored using high-resolution numerical simulations in order to more accurately quantify sensitivities of the divergence calculation to the number of ships and their locations.

Besides rawinsondes, in-situ and remote sensing instrumentation will be installed at BCO and on-board the ships. Instruments such as lidar, radar, radiometers or cellometers will provide additional observations of clouds, aerosols, surface turbulence and air-sea fluxes of heat and moisture, and surface and boundary-layer properties. A scanning, S-band, radar operated by the Barbados Meteorological Service can be used for research purposes in the absence of severe weather. It will help characterize the mesoscale organization of convection, and the vertical structure of the shallow cloud cover (Nuijens et al, 2009; Oue et al, 2016). The possible deployment of a second C-Band radar, the POLDIRAD of the Institut für Physik der Atmosphäre at the Deutschen Zentrum für Luft- und Raumfahrt, is also being considered. Shipboard deployment of drones and a HeliKite, capable of large-airborne payloads, can be used to characterize aerosols and cloud microphysical properties. Laser-based spectrometers could measure the isotopic composition of water and provide an additional characterization of the balance between convective drying and turbulent moistening in the boundary layer, and simple instruments such as ceilometers will aid the characterization of the vertical distribution of clouds in the observational domain.

The ships will also provide an opportunity to characterize the state of the upper ocean and more specifically the mesoscale ocean eddies which are particularly frequent east of Barbados (section 5.2). Beyond their importance for the ocean transport, mesoscale ocean eddies are increasingly recognized as influencing air-sea fluxes and clouds. This raises the question as to whether they might play a role in the organization of shallow cumulus clouds. Oceanographic measurements of the vertical profiles of temperature, salinity, pressure, oxygen and other biogeochemical properties of the upper ocean through in-situ sensors or profiling instruments, combined with the deployment of Argo profiling floats and autonomous observing platforms such as gliders or wave-gliders, would provide an unprecedented characterization of tropical mesoscale ocean eddies and would foster studies of their impact on clouds (section 5.2).

2.3 Satellite observations

To complement the airborne measurements, we will coordinate field operations with overpasses of several satellites: the Advanced Spaceborne Thermal Emission and Reflection Radiometer (ASTER), an imaging instrument with 15 m spatial resolution on-board Terra, plus a number of satellites from flagship space missions that we expect to be in orbit by the time of the campaign: *ADM-Aeolus* (whose launch is planned by the end of 2017) will provide the first space measurements of radial wind profiles; *EarthCare* ((Illingworth et al, 2015), whose launch is scheduled in 2019), includes a Doppler cloud radar and a HSR lidar almost identical to those on board the ATR-42 which can provide a thorough characterization of clouds and aerosols from space; and *Megha-Tropiques* (Roca et al, 2015, launched in 2011 and whose mission has been extended until 2021) measures radiative fluxes at the top of the atmosphere, the vertical distribution of relative humidity through the troposphere, and precipitation as part of the GPM (Global Precipitation Measurement) mission.

Shallow cumulus clouds exhibit a large range of mesoscale organizations from seemingly randomly-distributed cloud clusters, wind-parallel street lines or arcs (Figure 4). Space observations of the atmosphere at high spatial resolution such as derived from ASTER or other instruments (e.g. GOES, MISR or MODIS imagers), potentially complemented by radar observations from one

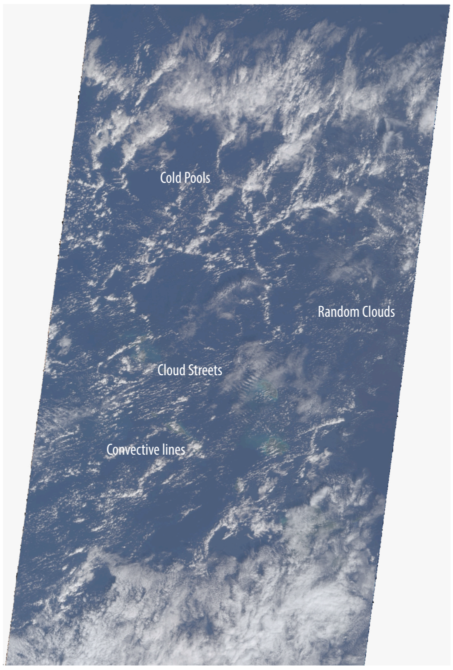

Fig. 4: Sample of cloud organizations observed during the RICO campaign from MISR satellite imagery.

of the Research Vessels (section 2.2) or from the land station, will be crucial to characterize the spatial organization of clouds within the area sampled by the aircraft missions. EUREC^{4}A will be the first field study to investigate whether this organization matters for the statistical properties of the shallow cumulus cloud field.

Satellite observations will provide further characterizations of the vertical structure of the atmosphere in terms of water vapor, clouds (section 3.2) and winds, and with measurements of radiative fluxes at the top of the atmosphere. Reciprocally, in-situ observations will be useful to evaluate the satellite remote sensing (section 4.2).

3 The premises

The experimental strategy of the EUREC^{4}A campaign rests on three main premises:

– The large-scale vertical motion on scales O(100 km) can be measured using dropsondes,
– The cloud fraction near cloud-base can be inferred from lidar-radar measurements

– The convective mass flux at cloud-base can be inferred from the subcloud layer mass budget.

In this section, we present arguments and results from ongoing analyses that show that the first of these premises appears sound, and we discuss how the other two are currently being tested, and how the experimental strategy might be adapted based on the outcome of these tests.

3.1 Using dropsondes to measure the large-scale vertical motion

A main component of the large-scale mass, heat and moisture budgets is the large-scale vertical velocity ω (Yanai et al, 1973). From the equation of mass continuity, ω can be derived from the divergence, D of the horizontal wind $\mathbf{V}$ ($D = \nabla \cdot .\mathbf{V}$) as $\nabla \cdot .\mathbf{V} + \frac{\partial \omega}{\partial P} = 0$ where P is the atmospheric pressure. D and ω are known to strongly influence the properties of the trade-cumulus boundary layer and low-level cloudiness (e.g., Albrecht et al, 1979). Our ability to measure these two quantities during EUREC^{4}A will thus critically determine the success of the campaign.

Measurements of the large-scale vertical motion on the time and space scale of individual airborne observations has long been recognized as being essential to understand how cloudiness develops and to calculate the heat and moisture budgets of the lower troposphere, but so far generally thought to be impossible. During ATEX and BOMEX, attempts have been made to estimate the large-scale divergence from rawinsonde sounding networks and/or aircraft data at a particular level using the "line integral" method (Holland and Rasmusson, 1973; Nitta and Esbensen, 1974b). It infers D from horizontal wind measurements using:

$$D = \frac{1}{A} \oint V_n \, dl, \tag{1}$$

where V_n is the component of the horizontal wind normal to the perimeter of measurements, and A is the area of the region enclosed by it. When applied to aircraft measurements, this method requires a stationary wind field and perfectly closed flights.

An alternative method, referred to as the "regression method', has been proposed by Lenschow et al (2007) and successfully applied to DYCOMS-II data. It assumes a particular model for the wind-field, but can be more easily adopted to a wider range of sampling geometries. Lenschow et al (2007) assumed that wind variations in longitude, latitude and time are linear for each vertical level, such that:

$$\mathbf{V} = \mathbf{V_o} + \frac{\partial \mathbf{V}}{\partial x} \Delta x + \frac{\partial \mathbf{V}}{\partial y} \Delta y + \frac{\partial \mathbf{V}}{\partial t} \Delta t, \tag{2}$$

where $\mathbf{V_o}$ is the mean wind velocity over the area, Δx and Δy are the eastward and northward displacements from a chosen center point. Δt is the change in

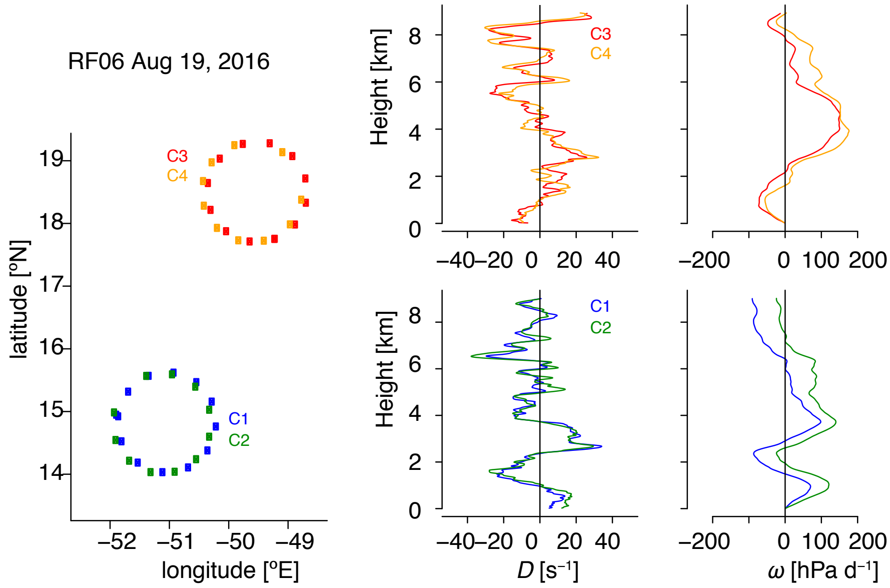

Fig. 5: (left) Research flights performed during NARVAL2 on Aug 19th and the vertical profiles of large-scale mass divergence D and large-scale vertical velocity ω derived from the dropsondes measurements for each circle.

time relative to a reference, for instance the mid-point time of the sampling. An approximate solution of this overdetermined system can be found by computing the coefficients of a least squares fit to the wind field defined as (2). By measuring $\mathbf{V}$ and solving (2) for its gradients, D can then be computed as: $D = \frac{\partial u}{\partial x} + \frac{\partial v}{\partial y}$.

So far, this methodology has been applied to wind measurements from rawinsondes or flight-level estimates of winds from an aircraft gust probe. Wind measurements from GPS dropsondes (Wang et al, 2015) now offers the opportunity to measure the vertical profiles of D and ω during airborne field campaigns. However, this methodology needs to be evaluated. In particular it has to be checked whether the divergence measured in this way would actually represent the large-scale circulation or would instead be noisy and dominated by short-term features unrelated to the large-scale environment.

To answer this question, this methodology was tested during the NARVAL2 campaign, which consisted of ten research flights of HALO, and took place in the EUREC^{4}A target areas, upwind of Barbados, during August 2016. Two of the HALO flights during NARVAL2 were specifically designed as a pilot study for the proposed EUREC^{4}A divergence measurements. During the two research flights RF03 and RF06 (carried out on 12 and 19 August 2016), HALO flew horizontal circles of 45-48 minutes (160 km diameter) at an altitude of 9 km. Dropsondes were released intensively along each circle. The dropsonde system on HALO can only track four sondes simultaneously. When this capability was combined with the fall time of an individual dropsonde (about 12 min for a sonde to fall from 9 km to the surface) it implied a period of about four minutes between sonde launches, resulting in the possibility of up to twelve sondes launches, equally spaced, over an interval of about 45 minutes. The dropsondes (Vaisala RD94) measured the vertical profiles of pressure, temperature and humidity with an accuracy of 0.4 hPa, 0.2 °C and 2 %, respectively. Equipped with a GPS receiver, the dropsondes also measured the horizontal wind speed with an accuracy of 0.1 m.s^{-1}.

To test the method, pairs of circles were flown in the same air mass (one clockwise, one counter-clockwise, the center of the second circle slightly drifted with the mean wind relative to the first one). The idea was that if the wind-field was sufficiently stationary, and the measurements by the sondes were physical, one would expect similar answers to arise between a pair of circles flown in the same airmass. As shown on Figure 5, the vertical profiles of D and ω derived for each circle of a given pair exhibit a consistent and reproductible vertical structure over most of the troposphere. Differences between circles of a given pair awillre much smaller than differences from one pair to the next, where different pairs of circles were spatially dislocated. The vertical structure of D and ω measured by dropsondes in the lower troposphere (below 4 km), such as the maximum subsidence near the top of the mixed layer, is qualitatively consistent with that measured by rawinsondes or aircraft measurements during previous field campaigns in the trades (Holland and Rasmusson, 1973; Nitta and Esbensen, 1974b). It is also in good agreement with the vertical structure of D and ω derived over the area from ECMWF operational forecasts during periods where the horizontal wind of the forecasts is in good agreement with the dropsondes, and with high-resolution forecasts run by a Cloud-Resolving Model initialized by ECMWF analyses (not shown). It shows therefore that dropsondes can actually be used to measure the vertical profiles of D and ω on scales of O(100 km) and to discriminate the spatial heterogeneity of the environment.

Three further issues are currently being explored, also in combination with high-resolution simulations which will be used to emulate different sounding strategies: (1) The minimum number of sondes to be dropped along each circle to reach equivalent results, (2) the spatial scale over which the large-scale dynamics best correlates with the macrophysical cloud properties, and (3) the influence of vertical shear of the horizontal wind, which is much more pronounced during the winter season. Depending on the result of these investigations, the number of sondes to be dropped, as well as the size of the circular flights to be flown during EUREC^{4}A will be optimized.

3.2 Estimating the near-base cloud fraction from aircraft measurements

An additional important and novel element of the EUREC^{4}A strategy will be to measure the cloud fraction just above cloud base (around 1 km). Measuring the cloud fraction has always been a challenge from an observational point of view, in particular in the trades where the cloud field is low, broken and composed of small clouds. This makes it difficult to use passive satellite observations unless the remote sensing is very sensitive to the presence of cloud droplets, and has a high horizontal and vertical resolution.

Measurements of cloud-fraction at cloud-base are important for understanding what processes control its variations in the current climate and to test some of the processes involved in the climate change cloud feedbacks of climate models. For this purpose, the Leandre New Generation (LNG) lidar (Bruneau et al, 2015) and the Bistatic Radar System for Atmospheric Studies (BASTA) radar (Delanoë et al, 2016) on-board the ATR42 flying just above cloud base will acquire dedicated horizontally pointing observations from the aircraft windows. At this level, LES simulations (e.g., vanZanten et al, 2011; Vogel et al, 2016) suggest that the relative dryness of the atmosphere combined with the relatively low cloud water content (Figure 6) should maximize the range of the lidar measurements, thereby providing useful backscatter signal over a distance of about 10 km, thus greatly enhancing the sampling volume. Beyond the mean cloud fraction, the lidar-radar measurements will help determine the spectrum of cloud sizes at cloud base, which is thought to be a crucial information for understanding the coupling between the subcloud-layer and the cloud layer (Neggers, 2015).

The feasibility of this approach will be tested using LES simulations and by applying to LES outputs the McRALI (Monte Carlo Radar and LIdar) simulator of the lidar and radar instruments on board the ATR42 (and satellite platforms). McRALI is a forward Monte Carlo model (Cornet et al, 2010) enhanced to take into account light polarization, multiple scattering, high spectral resolution, Doppler effect and the three-dimensional structure of the cloudy atmosphere (Szczap et al, 2013, Alkasem et al., in preparation). By diagnosing the cloud fraction that the lidar and radar would measure if they were probing an atmosphere similar to that simulated by the LES model, we will assess how well the above approach can work, and/or whether the experimental strategy will have to be revised to get more accurate measurements of the cloud-base cloud fraction.

Beside the cloud base information, it will be important to determine the vertical profile of cloud fraction, the cloud fraction at cloud top in particular. Indeed the cloud fraction near the inversion level appears to be more variable than that at cloud base (Nuijens et al, 2014), varies strongly with the intensity of the convective mass flux (e.g., Brient et al, 2016; Vial et al, 2016) and strongly influences the variations of the total cloud cover (Rodts et al, 2003). Different methodologies will be tested to retrieve this information from observations. One will consist in analyzing the vertical distributions of the lidar backscatter signal and radar reflectivities measured from the downward looking instruments on HALO and the upward and downward looking instruments on the ATR-42. Another will consist in analyzing data from ground or ship-borne instruments. Ceilometers will be very useful, but a scanning radar (Oue et al, 2016) on one of the research vessels or deployed on Barbados is also

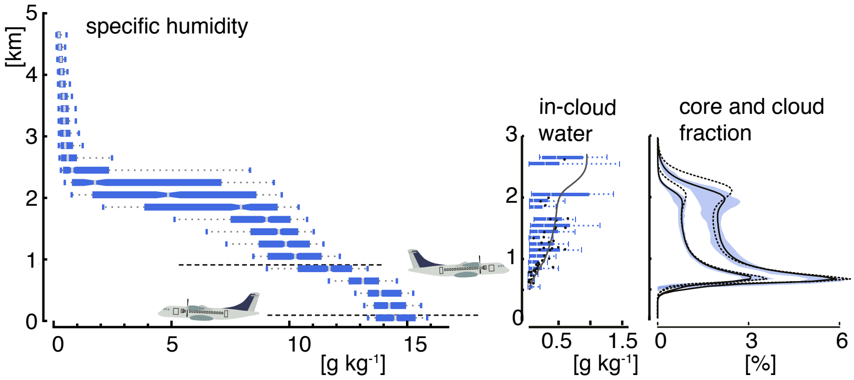

Fig. 6: Vertical profiles of water vapor mixing ratio (left) from the NARVAL 1 flights, (middle) condensed water (q_l) and (right) cloud fraction from RICO. The NARVAL 1 water vapor is derived from all sondes for which surface air temperatures exceed 25 °C, as measured east of Barbados in December 2013. The distribution is described by the box plots showing range (5-95 %), interquartile and median. Cloud condensate profiles are for similar conditions but during RICO and adapted from vanZanten et al (2011). Flight date is characterized by box plots (interquartile and 5-95 %) and dots (flight averaged). The line is the ensemble mean of 12 large-eddy simulations. Cloud and cloud core fraction profiles are derived from LES simulations (adapted from vanZanten et al, 2011). Ensemble (inter-quartile) spread among LES simulations is given by the shading, and the mean profiles from non-precipitating simulations are shown by the thin dashed line. Proposed flight levels of ATR-42 are also illustrated.

being considered. Yet another approach will consist in analyzing observations from the SpecMACs instrument on HALO. SpecMACs is a hyper-spectral line-imager with a field of view of about 40° which allows to map a 10 km swath with 10 m resolution, this swath being similar to the anticipated one for the sideways staring lidar on-board the ATR-42. Oxygen A-band measurements from SpecMACS can be used to measure the distance to the cloud top. Finally, satellite measurements such as those from lidar (Calipso, Winker et al, 2003, and/or EarthCare) or high-resolution spectrometers such as ASTER, which has a 15 m horizontal resolution and many channels in the infrared, visible and near-infrared (Zhao and Di Girolamo, 2007), will provide independent estimates of the vertical profile of cloud fraction. However, when comparing in-situ estimates of the cloud fraction with those from passive satellite remote sensing, some geometric constraints will have to be considered since along-track aircraft measurements provide estimates that may differ from areal satellite retrievals (Rodts et al, 2003).

The dynamic properties of clouds will be infered from radar measurements (e.g. vertical velocities at cloud base will help determine whether a cloud is active or passive), and the microphysical properties will be derived from the combined analysis of radar-lidar measurements, passive radiometers and in-situ measurements. In-situ data could be collected by small unmanned aircraft launched from the ships or the island (e.g. drones) as well as a tethered HeliKite capable of carrying payloads of up to 50 kg to heights of 3 km. In addition the ATR-42 will have a nominal package of basic cloud microphysical probes for characterizing the droplet spectrum and cloud liquid-water contents. Vertically-integrated cloud liquid content of shallow clouds will be measured using downward looking radiometers flown aboard HALO. The occurrence of precipitation and mesoscale organization of precipitating shallow clouds will be characterized from the scanning precipitation (S-band) radar on Barbados, and may be complemented by a scanning C-band system.

Finally, measuring the radiative effects of clouds will be critical to assess the coupling between clouds and their large-scale environment. Vertically-integrated estimates will be derived from broadband radiative fluxes measured near the surface and in the upper troposphere, and vertical profiles of the radiative heating rate will be inferred from radiative transfer calculations using observed atmospheric and cloud properties.

3.3 Inferring the convective mass flux from the subcloud layer mass budget

To test the hypothesis that lower-tropospheric mixing critically influences the trade-cumulus cloud fraction at cloud base (e. g., Rieck et al, 2012; Gettelman et al, 2012; Sherwood et al, 2014; Brient et al, 2016; Vial et al, 2016), we will need to measure the strength of the convective mixing or quantities closely related to it. Several measures have been proposed for this purpose, which often depend on the convective mass flux at cloud base and/or the vertical profiles of humidity, temperature or moist static energy.

During EUREC^{4}A, we propose to estimate the convective mass flux at cloud base, M, from the mass budget of the sub-cloud layer. The mass budget of the sub-cloud layer can be expressed as:

$$\frac{\mathrm{d}\eta}{\mathrm{d}t} = E + \overline{w_\eta} - M. \tag{3}$$

η represents the depth of the sub-cloud layer, E is the top entrainment velocity, $\overline{w_\eta}$ is the large-scale vertical velocity at η (which is related to ω at the same level by a coordinate tranformation) and M is the convective mass flux (divided by the air density) out of the sub-cloud layer. This budget is illustrated in Figure 7. LES of precipitating shallow trade-wind convection have been used to test the feasibility of estimating M as a residual of the remaining terms in Eq. 3. The LES are performed with homogeneous large-scale forcings on a 50x50x10 km^3 domain that supports the emergence of deeper and organized shallow convection (Vogel et al, 2016).

Whereas $\overline{w_\eta}$ is directly given by the large-scale subsidence profile of the LES, in analogy to what is proposed for the EUREC^{4}A measurements, E

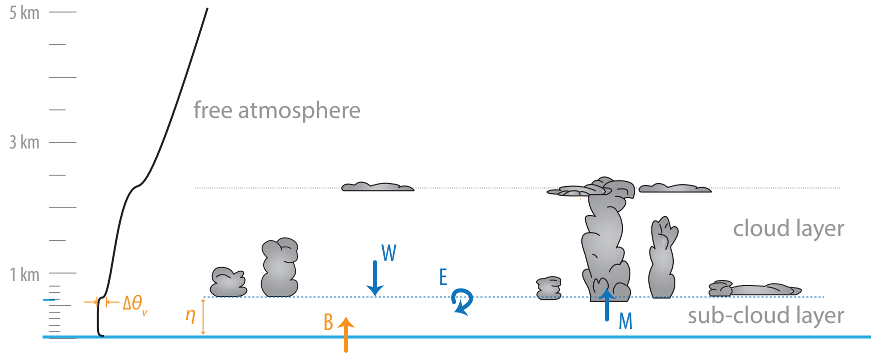

Fig. 7: Schematic representation of the subcloud-layer and of the main physical processes affecting its mass budget.

is estimated from the buoyancy flux at the surface, B, which parameterizes the entrainment buoyancy flux ($\left(\overline{w'\theta_v'}\right)_\eta = a\,B$), where a is a proportionality constant. By combining this estimate of the entrainment buoyancy flux with the vertical jump in virtual potential temperature (θ_v) across the transition layer (Siebesma and Cuijpers, 1995; Siebesma et al, 2003) it is possible to estimate E as: $E = -\left(\overline{w'\theta_v'}\right)_\eta / \Delta\theta_v$. The denominator, and the constant a, are estimated by fitting a mixed layer to the θ_v profile of the LES, with the uniform θ_v of the mixed layer chosen to match the integrated θ_v of the original profile. $\Delta\theta_v$ is the jump between the mixed layer θ_v, and θ_v at the top of the mixed-layer.

A preliminary analysis of large-eddy simulations representative of typical trade-cumulus conditions (Vogel et al, 2016) shows that estimating M in this manner agrees reasonably well (within 35% for the initial calculations) with the value that is diagnosed directly from model output of cloud-core vertical velocity and cloud-core area fraction. The quantitative consistency between both estimates is sensitive to the definition of η in the LES (both the maximum gradient in total humidity or the local minimum in the vertical velocity variance close to cloud base are suitable definitions), and on how the buoyancy flux at the top of the sub-cloud layer relates to the surface buoyancy flux. By the time of the EUREC^{4}A field campaign, the present method will be refined by defining η such that the estimated and diagnosed mass fluxes are in closer agreement (η can be defined in several ways), and by accounting for the small temporal fluctuations in η. We will also investigate how much the method can capture the sensitivity of the mass flux to different boundary conditions such as sea surface temperature, wind speed and the large-scale divergence D, which are associated with different precipitation fluxes and different degrees of convective organization.

This estimate of the cumulus mass flux inferred from the mass budget of the subcloud-layer will be compared with estimates from two alternative methods. One method will consist in estimating M from the energy budget of the

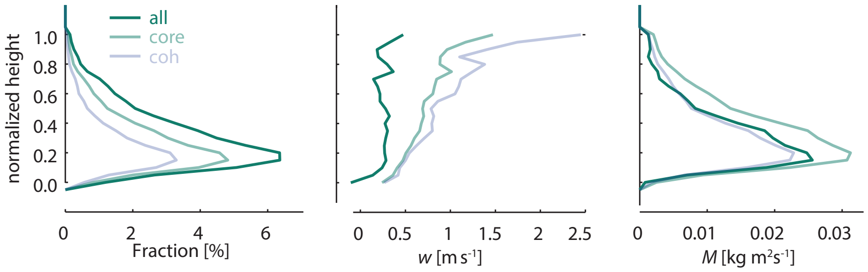

Fig. 8: Boundary-layer profiles (normalized by the maximum cloud top height and minimum cloud base height) of hourly averaged (a) cloud fraction, (b) vertical velocity and (c) mass flux for all, core and vertically coherent updraft samples collected at the island of Graciosa in the Azores. (Adapted from Ghate et al, 2011).

subcloud-layer: from measurements of surface turbulent enthalphy fluxes, of the large-scale vertical velocity at the top of the subcloud layer ($\overline{w_\eta}$), of the vertical jump in moist-static energy at the top of the subcloud layer, and of the radiative cooling rate within the subcloud layer, it will be possible to infer M from the conservation equation of the subcloud-layer moist static energy. Another method will consist in estimating M using radar measurements from the ATR42 flying just above cloud base. Based on vertical velocity measurements within clouds ($w_{\rm cld}$), the fractional area covered by active clouds ($a_{\rm cld}$) will be measured. The cloudy mass flux (divided by the density of air) will then be estimated as: $M = a_{\rm cld} \cdot w_{\rm cld}$ (e.g. Kollias and Albrecht, 2010; Ghate et al, 2011; Lamer et al, 2015; Ghate et al, 2016). The cloudy area (as well as properties within it) can be decomposed further into updraft and downdraft areas, or even further into different cloud parts (e.g. core or vertically-coherent updraft, Figure 8), or into a spectrum of cloud sizes (Neggers, 2015). Similar and ongoing measurements of M from the cloud-radars at the Barbados Cloud Observatory will provide additional context for these measurements, as during EUREC^{4}A it is intended to target airmasses upwind of the observatory.

The comparison of these different methods for estimating the cumulus mass flux will help to assess the robustness of the estimates, especially regarding the sensitivity of the mass flux variations to changes in environmental conditions. Note that these estimates will also help determine whether in the subcloud-layer the surface enthalphy fluxes are compensated mostly by clear-air entrainment or by convective mass fluxes (Thayer-Calder and Randall, 2015), which will help test the convective mass flux closure hypotheses of the cumulus parameterizations used in weather and climate models (Arakawa and Schubert, 1974; Emanuel, 1989; Raymond, 1995).

4 A benchmark dataset

Previous reference observations for linking clouds to circulation in the trades are BOMEX, ATEX and GATE. These are field studies which took place nearly a half century ago before the advent of satellite remote sensing, not to mention transformative progress in simulation science. Through a close integration with satellite remote sensing and advances in modeling, EUREC^{4}A aims to provide a reference data set for studying clouds and circulation in the trade-wind region.

4.1 A simulation and modelling testbed

LES models have long been used to simulate trade-cumulus clouds. Nowdays, they are run over increasingly larger domains, which allows shallow convection to organize (e.g., Seifert and Heus, 2013; Vogel et al, 2016). The apparent realism of the circulations and clouds that develop often encourages their adoption as an adequate description of reality. However, LES incorporates approximations and assumptions beyond the idealizations in the set-up employed. These include the numerical methods adopted, which are known to significantly affect cloud structure and fraction (see Vial et al., this volume), as well as the way in which radiative transfer, cloud microphysics and small-scale turbulent motions are parameterized. Critical tests of the LES representation of cloud fields as a function of their large-scale environment have only been performed for a very few cases, and not in conditions of shallow cumulus. Most of the evaluations have been using observational data from ATEX, BOMEX or RICO (Stevens et al, 2001; Siebesma et al, 2003; vanZanten et al, 2011). These observations make it possible to evaluate carefully the thermodynamic structure of the boundary layer for a limited set of given large-scale forcings. However they do not allow to answer critical questions such as: What is the typical cloud cover and what is the fraction of the cloudy air that is positively buoyant? How strong is the cumulus mass flux at cloud base? How does the cloud fraction and cloud water content vary with synoptic changes in large-scale vertical motion, surface conditions and convective organization? By providing estimates of the cumulus mass flux, of the large-scale vertical velocity, and of the large-scale environment, the EUREC^{4}A campaign will offer opportunities to answer some of the above-mentioned questions and to evaluate LES simulations of shallow cumulus beyond previous investigations.

One process of particular interest, is the cumulus "valve-mechanism" for regulating cloud-base mass fluxes (e.g., Neggers, 2015). This mechanism suggests that the mass flux is that required to maintain the cloud-base cloud-fraction nearly constant. During EUREC^{4}A we will be able to evaluate to what extent it is operative, and the degree to which this indeed controls cloud base cloud fraction. Another question is to what extent mesoscale variability, which may often be the flow 'debris' of much larger-scale circulations not represented by LES, is important for determining cloudiness and its variability. For instance, the influence that cold pools or surface temperature heterogeneities associated with sub-mesoscale processes in the ocean (section 5.2), may exert on cloudiness remains an open issue.

In addition to helping evaluate and improve LES, EUREC^{4}A will also help evaluate the physics of large-scale climate and weather models. As discussed in section 3.3, a better understanding and assessment of the different contributions to the subcloud-layer energy budget will help assess the hypotheses underlying the cumulus mass flux closures used in convective parameterizations. Moreover, large-scale models still exhibit significant biases in the representation of clouds and circulation in the trades. For instance, most models over-estimate the reflection of solar radiation by trade-cumulus clouds despite an under-estimate of the cloud fraction and/or the cloud water (the so-called 'too few, too bright' problem, Karlsson et al, 2008; Nam et al, 2012). Models also exhibit persistent biases in their simulation of the surface wind stress (Wang and Carton, 2003; Simpson et al, 2014), which can relate to wrong representations of the surface drag and/or of the momentum transport by shallow convective clouds (Polichtchouk and Shepherd, 2016; Schlemmer et al, submitted). The comparison with EUREC^{4}A observations of short-term forecasts run with such models will help disentangle sources of model errors in the representation of physical processes and their interaction with the large-scale circulation.

By computing large-scale forcings (water vapor and heat large-scale advections) from EUREC^{4}A observations, it will also be possible to run single-column versions of large-scale models (Single-Column Models or SCMs). It will help to test the model physics further, and also to better understand the cloud feedbacks produced by these models. Indeed there is ample evidence that single-column simulations of shallow cumulus clouds can help understand low-cloud feedback processes and their dependence on process representations (e.g., Brient and Bony, 2012, 2013; Zhang and Bretherton, 2008; Zhang et al, 2013; Dal Gesso et al, 2015; Brient et al, 2016). The link to observations, and the comparison between LES and SCM simulations, will allow to investigate the relationship between the response of shallow cumulus clouds to prescribed climate change perturbations and the realism of the simulated clouds in the present-day climate, which will help answer questions such as: How does the cloud cover depend on the strength of convective mixing? How variable is it with changes in environmental conditions? Is it possible to constrain the strength of climate change low-coud feedbacks from present-day processes? (Vial et al., this volume). Taken all together, the new experimental methodologies being developed and deployed as part of EUREC^{4}A will provide new opportunities to provide a reference data set to inform modelling and simulation of shallow cumulus clouds.

4.2 A remote sensing testbed

Observations from field campaigns are not only fundamental to investigate the physics of trade-cumulus clouds but also to test, and eventually improve, the instruments and algorithms of remote sensing that are used to observe the Earth from space. Beyond the evaluation of cloud retrievals from current satellites, EUREC^{4}A is expected to contribute to the evaluation of the cloud and wind retrievals from two new flagship satellite missions of the European Space Agency: ADM-Aeolus and EarthCARE, that will provide unprecedented information on clouds and circulation.

Remote sensing in based on the capability to infer remote properties by analysing how atmospheric particles or molecules interact with radiation at specific wavelengths. During EUREC^{4}A, the instruments onboard HALO and the ATR42 aircraft will sample almost the full spectrum of wavelengths of atmospheric electromagnetic radiation (including UV, solar to thermal infrared, radar and microwave wavelengths), making it possible to retrieve a wide range of geophysical properties. Moreover, some of the instruments onboard the aicraft will be almost identical to those used on ADM-Aeolus and EarthCARE satellites (e.g the UV HSR Doppler wind Lidar operating at 355 nm or the 95 GHz doppler cloud radar). When flying along satellite orbits, it will thus be possible to make direct comparisons between airborne and space measurements. The in-situ observations will help interpret the remote sensing in terms of geophysical variables, and the comparison between airborne and space measurements will help evaluate some of the limitations of the satellite remote sensing.

The main limitations of remote sensing are due to the lack of sensitivity of the sensors (which is of particular concern when probing the lower atmosphere from space, but much less from an aircraft), the inability to exploit some measurements near the surface (e.g. the blind zone arising from the contamination of radar measurements by ground clutter or from the saturation of the lidar signal) and the poor spatial resolution of the measurements (which is particularly problematic in areas covered by small broken clouds such as shallow cumulus fields). For passive measurements, which have the best spatial coverage, a particular challenge is identifying sufficiently unique information to unravel the atmospheric vertical structure from signals that necessarily integrate over this structure. The synergy of in-situ, airborne and space measurements made in coincidence during EUREC^{4}A, jointly with high-resolution simulations from weather forecast models and LES simulations of the campaign area, will help quantify these different sources of uncertainty and test some of the hypotheses used in the cloud or wind retrieval algorithms. A few examples are given below.

Satellite instruments like MODIS or MetOP measure radiances in different wavelength channels, and these measurements are used to retrieve cloud droplet number, cloud phase, optical thickness, and droplet or particle size at cloud top at a spatial resolution of about 1 km. This resolution is insufficient for the observation of shallow cumulus clouds. The specMACS instrument onboard

HALO (Appendix A), which combines hyper-spectral wavelength resolution in the visible and near-infrared wavelength range with a spatial resolution of a few 10 m, will allow to observe shallow cumulus clouds in much more details. Obvious products will be cloud cover and cloud size distributions. In addition, the use of three-dimensional radiative transfer methods will allow to retrieve cloud optical thickness, droplet radius, and cloud top structure with high spatial resolution (Mayer, B., 2009; Zinner et al, 2006), even distinguishing the cloud core area from the optically thinner edges. The contribution of clouds to solar heating and infrared cooling rates will also be estimated from these parameters.

Another key property of clouds for which satellite retrievals remain very uncertain is the cloud liquid water path (LWP). Most of today's knowledge on the global distribution of cloud liquid water is derived from polar orbiting satellites that measure radiances in the thermal infrared and microwave spectral regions. However, given the coarse spatial resolution of these measurements (several tens of kilometers), the LWP retrievals critically depend on the estimated cloud fraction (Horváth and Gentemann, 2007) and cloud vertical structure (Borg and Bennartz, 2007). The synergy of the different instruments onboard the two aircraft will provide fine scale information on the variability of water vapor, liquid water and cloudiness over an area of 200x200 km which will help evaluate satellite retrievals and the validity off their underlying assumptions. The combination of active and passive microwave radiometry will also allow to detect the amount of drizzle and precipitation in shallow cumulus cloud fields. Beyond its intrinsic interest, this detection will make it possible to test the validity of the precipitation thresholds used in LWP retrievals (Wentz and Spencer, 1998), and thus to improve LWP retrievals in trade-wind regions.

Active satellite remote sensing provides observations along narrow curtains aligned with the flight track. To achieve radiative closure (as envisioned with EarthCARE) or to generate precipitation fields (as done as part of the GPM mission), it is crucial to combine curtain measurements with observations from wide swath instruments. For this purpose, LES simulations are often used to get statistical information about the three-dimensional structure of the cloudy atmosphere. By providing the reference dataset necessary to assess such statistics (section 4.1), EUREC^{4}A will thus help assess and improve these techniques.

Finally, the LNG (lidar) instrument onboard the ATR42 will have the capability to mimic ADM-Aeolus measurements: the 355 nm HSR doppler wind lidar of the satellite will point 35 deg from nadir (orthogonal to the ground track velocity vector to avoid contribution from the satellite velocity) to derive profiles of the horizontal wind component, and will also regularly point to nadir for calibration. LNG measurements along the satellite orbits and in the same viewing direction, together with in situ measurements and other airborne observations, will help evaluate the L2A (cloud and aerosol optical properties) and L2B (radial winds) ADM-Aeolus products over distances of several hundreds of kilometers.

5 An opportunity for complementary scientific objectives

The intensive observations of the atmosphere and of the surface that will be collected during EUREC^{4}A campaign will provide an opportunity to address additional scientific issues. Two of them are mentioned below, but many more could arise over the next years.

5.1 Rectification of large-scale vertical motions by the diurnal cycle of shallow clouds

In addition to complementing and providing vital large-scale context for the aircraft missions, measurements by the large-scale sounding array will help answer scientific questions such as: What is the role of transient disturbances and their influence over large-scale vertical motion in modulating convective mass flux and large-scale diabatic heating? What drives the diurnal cycle of vertical motion and clouds in the trades?

Mounting evidence indicates that the Hadley cell over the remote oceans is characterized by a pronounced, regular diurnal cycle in overturning motion, quite distinct from the influences of land (Nitta and Esbensen, 1974b; Gille et al, 2003; Wood et al, 2009). It is possible that this diurnal cycle owes fundamentally to the response of deep convective clouds in the ITCZ to the diurnal cycle of direct shortwave absorption (Nitta and Esbensen, 1974a), although this topic is unresolved. Observations from suppressed regimes in the Indian Ocean warm pool region reveal that the diurnal cycle in large-scale vertical motion is intimately tied to a diurnal cycle in the shallow convective-cloud population: clouds deepen each afternoon as subsidence relaxes, while the afternoon increase in more active, precipitating clouds leads to more cold pools that in turn augment cloud area fraction (Ruppert and Johnson, 2015, 2016). Experiments conducted with a LES framework suggest that this diurnal cloud feedback between large-scale vertical motion and macroscopic cloud properties augments diabatic heating, thus impacting large-scale circulation, on longer time scales through nonlinear rectification (Ruppert, 2016).

An additional objective of EUREC^{4}A will therefore be to diagnose the relationships between radiation, clouds, and large-scale vertical motion on the diurnal time scale, and to relate this time scale to other modes of variability. The target hypothesis pertaining to this process is that the diurnal shortwave heating cycle drives a diurnal cycle of deep convection in the ITCZ, which in turn drives a diurnal cycle of large-scale overturning motion in the greater Hadley cell.

5.2 Ocean eddies

The ocean is a fundamentally turbulent fluid full of fine-scale structures such as eddies, fronts, jets and filaments (McWilliams, 2016). These oceanic structures, grouped as mesoscale (10-500 km, 10-100 days) and submesoscale (few

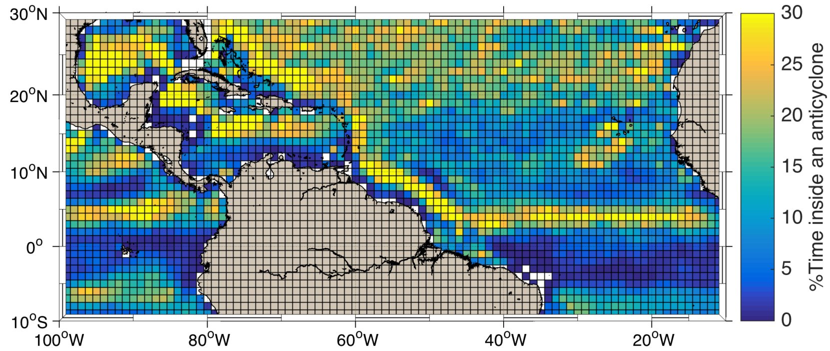

Fig. 9: The route of ocean eddies. Statistics of ocean mesoscale eddies derived from satellite altimetry (shown is the fraction of the time inside an anticyclone).

hundreds of meters, daily time-scales) dynamics, are recognized as key contributors to the ocean circulation (e.g., Zhang et al, 2013). There is also increasing evidence that they impact air-sea interactions and influence the winds and clouds of the overlying atmosphere (Chelton et al, 2004; Ferreira and Frankignoul, 2008; Frenger et al, 2013; Byrne et al, 2015). However, few observations are available to quantify the role of ocean eddies in the transport of water properties and in air-sea interactions, especially in the tropics.

Automatic eddy detection from satellite observations show the presence of intense warm ocean eddies (i.e., anticyclonic eddies) in the western tropical Atlantic (Laxenaire et al, in preparation), especially along Guiana, Caribbean currents and along the North Equatorial Current which all meet just east of Barbados (Fig 9). The EUREC^{4}A campaign, which will take place right in this area, thus provides an opportunity to study the properties of ocean eddies and their role in the interactions between the ocean and the atmosphere at the mesoscale. More specifically, the extensive set of atmospheric observations combined with oceanographic measurements will allow to address questions such as: What is the role of ocean mesoscale eddies in modyfying atmosphere-ocean coupling and in influencing the mesoscale organization of the atmosphere and shallow clouds in particular?

This issue will be addressed by completing the atmospheric measurements of EUREC^{4}A with oceanographic measurements. The most interesting ocean mesoscale features will be identified from near real-time satellite altimetry data (AVISO Ssalto/Duacs), and then one of the ships will be used to deploy oceanographic instruments around them (e.g. within anticyclonic eddies) while a second ship will characterize the surrounding background field. In both areas, ocean vertical profiles of temperature, salinity, pressure, oxygen, and other biogeochemical properties (e.g. carbon related quantities) will be measured by a deep-reaching classical CTD (conductivity, temperature, depth) rosette, Argo profiling floats (that will be deployed within anticyclonic eddies within the Guiana and North Equatorial currents in the year preceding the EUREC^{4}A campaign), and possibly other autonomous observing platforms such as gliders and wave-gliders. More information about the instrumentation and the measurements envisioned is given in Appendix B. This strategy will be tested and refined before the campaign by undertaking a set of preliminary studies based on the analysis of data from satellites, Argo profiling floats, and eddy-resolving simulations of the ocean-atmosphere system.

5.3 Weather forecasting in the Caribbean

Through a close cooperation with the Caribbean Institute of Meteorology and Hydrology, EUREC^{4}A will also help test high-resolution modelling approaches to improve forecasts of high-impact weather. Heavy precipitation produced by severe weather associated with tropical storms, depressions and waves as well as those associated with strong localized convective systems frequently produce significant flash flooding and landslides on Caribbean islands that result in significant social and economic losses including loss of property and livelihoods and on occasion loss of life. Losses from such events can range from 25-200 percent of national Gross Domestic Product setting back national development by more than a decade in some instances. In order to reduce losses, in recent years there has been a significant effort to improve early warning hydrometeorological forecasts over the Caribbean. A critical step towards this goal has been the development of high-resolution (4 km) numerical weather forecasts using the Advance Research Weather Research and Forecasting (WRF) model. By providing a reference data set for the evaluation of cloud, turbulence and convective parameterizations, EUREC^{4}A will help improve the physics of the model, and eventually the quality of the rainfall forecasts.

Building national and regional resilience to increasing climate variability, climate change and extreme weather events in the Caribbean also includes increasing national and regional weather and climate data, related knowledge platforms and human capacity. By involving university students and other young scientists of the region in the field campaign and the longterm research activities related to it, EUREC^{4}A will help train the next generation of regional climate scientists and operational forecasters, develop databases that will facilitate the dissemination and use of the data collected in the area during field studies, and will promote international partnership and collaboration networks.

6 Conclusion

By characterizing for the first time both the macrophysical properties of trade shallow cumulus clouds and the large-scale environment in which convection and clouds are embedded, the EUREC^{4}A campaign will fill an observational gap and stands to make a high-profile contribution to climate science and meteorology. It should elucidate the role of convection and large-scale circulations in low-cloud feedbacks and thus address one of the central questions of the World Climate Research Programme's Grand Challenge on *Clouds, Circulation and Climate Sensitivity*. Through its alignment with two flagship ESA missions and the cutting-edge of modelling, it should also provide a new reference dataset which can be used to assess the modelling and the remote sensing for the years to come. The experimental strategy proposed for the campaign is ambitious. However, by analyzing observations from past campaigns and LES simulations of shallow cumulus fields, it will be tested and refined or revised if necessary, so as to maximize the chances of success.

A compact and well defined experimental strategy opens up the mission to international partners with complementary interests. This campaign should therefore be considered as an opportunity to nucleate a larger international efforts and to deploy additional investigations.

Appendix A: Aircraft instrumentation

Airborne platforms are one means to probe the thermodynamic, dynamic, and cloud properties of the atmosphere. At least two aircraft will participate in EUREC^{4}A, namely the French ATR-42 and the German HALO, and they will use complementary payloads. The HALO measurements aloft will characterize the large-scale (several thousands of km^2) environment in which clouds form, and the radjiative properties of the clouds therein. The ATR-42 measurements in the shallow cloud layer will constrain cloud macrophysical and microphysical properties, turbulent mixing processes and shallow circulations.

The airborne and in-situ measurements of EUREC^{4}A will also advance the evaluation and calibration of space measurements, and their interpretation in terms of geophysical variables (Wendisch and Brenguier, 2013). It will be the case in particular for observations from EarthCare and ADM-Aeolus, which are two flagship satellite missions of the European Space Agency's Living Planet Programme devoted to the observation of clouds and circulation, and whose measurements will be mimicked by several instruments on board both aircraft.

The ATR-42 aircraft and its instrumentation

The French ATR-42 is a bi turbo-prop aircraft from SAFIRE that has the capability of flying in the lower troposphere (ceiling at about 8 km) with a maximum range of about 1800 km. It will fly a series of low-level legs just above cloud base (around 1 km), about 100 km long and spaced by about 20 km, as a way to sample the cloud field within the area encompassed by HALO circles. A particularity of the aircraft instrumentation is that it will include sideways and vertical-pointing lidar and radars that will probe the atmosphere horizontally and vertically, aiming at measuring the cloud fraction at cloud base. The last leg before refueling will be flown below cloud level, to measure surface turbulent fluxes, temperature at the sea surface and in the sub-cloud layer, and near-surface radiation. Given the mean science speed of the aircraft (about 100 $\mathrm{m\,s^{-1}}$) and the endurance expected for the envisioned payload, the ATR-42 will make two four-hr flights per day bracketed by the daily nine-hr flight of HALO.

Instrument	Brief Description	Reference
Thermodynamics & turbulence	In situ water vapor, temperature, pressure and 3D wind; momentum and heat fluxes	
Cloud Particles	In situ liquid and total water contents; droplet size distribution (0.5-6000 μm); 2D particle imaging (25-6000 μm)	
BASTA Cloud Radar	Bistatic 95 Ghz Doppler cloud radar to be deployed in sidewards looking mode	Delanoë et al (2016)
RASTA Cloud Radar	Upward and Downward looking 95 Ghz Doppler cloud radar with six antenna configuration for wind-vector retrievals	Delanoë et al (2013)
LNG Lidar	Three wavelength (1064, 532 and 355 nm) high spectral resolution polarized backscatter lidar (sidewards, upwards or downwards pointing)	Bruneau et al (2015)
CLIMAT-AV	Three channel downward staring measurements of infrared irradiance at 8.7, 10.8, and 12.0 μm	Brogniez et al (2003)
Pyrgeometer	Hemispheric broadband upwelling and downwelling thermal infrared radiative fluxes	Kipp and Zonen CGR4
Pyranometer	Hemispheric broadband upwelling and downwelling solar radiative fluxes	Kipp and Zonen CMP22

Table 1: Synopsis of ATR-42 instrumentation

The ATR-42 will be equiped with advanced instrumentation including the multi-wavelength HSR backscatter lidar LNG (Bruneau et al, 2015), the 95 GHz Doppler radar RASTA (RAdar SysTem Airborne, Delanoë et al, 2013) and the mini cloud radar BASTA (Delanoë et al, 2016), three instruments developed at LATMOS[1] to characterize clouds, aerosol particles and hydrometeor particle velocities. Although RASTA will be observing the atmosphere above and below the aircraft, the HSR lidar and the BASTA Doppler radar will be staring sideways from the aircraft windows in order to measure the cloud fraction and cloud optical properties just above cloud base (section 3.2). In addition, the payload will include a thermal infrared radiometer (CLIMAT-AV, Conveyable Low-Noise Infrared Radiometer for Measurements of Atmosphere and Ground Surface Targets -Airborne Version) developed at the Laboratoire d'Optique Atmosphérique (Brogniez et al, 2003) to measure sea surface temperature, and hemispheric broadband pyrgeometer (Kipp and Zonen CGR4) and pyranometer (Kipp and Zonen CMP22) to measure upwelling and downwelling radiative fluxes in the longwave and shortwave, respectively. Finally,

[1] http://rali.projet.latmos.ipsl.fr, http://basta.projet.latmos.ipsl.fr

the aircraft will measure temperature, moisture and wind along its trajectory at a high frequency (25 s^{-1}) for turbulence statistics calculations.

The LNG airborne Lidar system is a three-wavelength (1064, 532, and 355 nm) backscatter lidar with polarization and high spectral resolution capability at 355 nm. It operates in a direct detection mode (measurement of the backscattered light intensity), which has the advantage of relying on both particulate and molecular scattering, and allows extended ranges and capabilities. Thanks to its two-wave interferometry system (Mach-Zehnder Interferometer) and its capability of High Spectral Resolution UV analysis, it can determine both optical parameters of aerosol and clouds and measurements of along-line-of-sight wind velocity, based on the Doppler effect on particles (Bruneau and Pelon, 2003; Bruneau et al, 2015). When scattering particles are moving, the wavelength of the scattered light is shifted by a small amount as a function of speed. The Doppler wind lidar measures this change of wavelength to determine the velocity of the wind in the direction of the light pulse. For a vertically pointing lidar, vertical velocity measurements are thus possible.

The BASTA (Bistatic Radar System for Atmospheric Studies) radar is a mini-cloud W-band radar (weighting only 32 kg) that measures the Doppler velocity and the reflectivity at 95 GHz (Delanoë et al, 2016). Its specificity, compared to traditional pulsed radars, it that instead of transmitting a large amount of energy for a very short time period (as a pulse), a lower amount of energy is transmitted continuously. The radar can be used in several modes depending on application, including 12.5m and 25m vertical resolution modes. The sensitivity of the instrument is about -40 dBZ at 1 km for 3-s integration and a range-gate of 25 m. Its unambiguous range is 12 km and 18 km for the 12.5 m and 25 m range-gate modes, respectively. The high mobility of the system allows to install the system with an horizontal pointing configuration. The most will be made of the bistatic nature of the system, with emitting and receiving radar signals through two side-by-side windows.

The RASTA (RAdar SysTem Airborne) radar measures the Doppler velocity and the reflectivity at 95GHz (W-band) along a radial defined by the pointing direction of the antenna (Delanoë et al, 2013). Depending on configurations, it can include 3 downward-looking beams (nadir, 28 degrees off-nadir and opposite the aircraft motion, and 20 degrees off-nadir perpendicular to the aircraft motion) and 3 upward-looking beams (zenith, 28 degrees off-nadir perpendicular to the aircraft motion, and 20 degrees off-zenith and opposite the aircraft motion). This unique configuration allows for the retrieval of the three-dimensional wind field, i.e. the three components of the wind on vertical plan below and above the aircraft when possible (6 antenna configuration), by combining the independent measurements of the projected wind vector on radar line of sights. The independent Doppler radial velocities are provided by the multi-beam antenna system. The radar range is 15 km, its vertical resolution is 60 m and its horizontal resolution ranges from 100 to 150 m depending on aircraft speed. RASTA measurements of vertical velocities within clouds, combined with lidar-radar estimates of the cloud fraction at cloud base, will help develop an estimate of the convective mass flux at cloud base that will be completely independent of the one derived from the analysis of the sub-cloud layer mass budget (section 3.3).

The CLIMAT-AV thermal infrared radiometer (Brogniez et al, 2003) measures (at nadir) radiances simultaneously in three narrowband channels centered at 8.7, 10.8, and 12.0 micron, with about 1 mm of full width at half maximum. It uses a 7-Hz sampling frequency and performs measurements within a 50-mrad field of view, which corresponds to a footprint of about 50 m at a 1-km range. CLIMAT-AV is very similar to the CALIPSO IIR system. The absolute accuracy of brightness temperature measurements is about of 0.1 K, and its sensitivity is of the order of 0.05 K. The radiances measured by CLIMAT-AV will be used to estimate the sea surface temperature.

The HALO aircraft and its instrumentation

The German high altitude and long-range research aircraft HALO is a modified Gulfstream G550 business jet with a long endurance (more than 10 flight hours), a long range (about 8000 km), and a high ceiling (15.5 km) (Wendisch et al, 2016). In cooperation with the DLR and the Universities of Cologne, Hamburg, Leipzig and Munich, it will be equipped with an extensive set of remote sensing instrumentation including: the differential absorption and high spectral resolution lidar system (WALES, Water vApour Lidar Experiment in Space), HAMP (the HALO Microwave Package) which includes the cloud radar MIRA36 (36 GHz) and a microwave radiometer, the spectral imager specMACS, and an instrument system that measures spectrally resolved upward and downward solar radiances and irradiances (SMART). The payload also includes in-situ measurements of the meteorological properties along the flight track (BAHAMAS), and the ability to launch dropsondes using the AVAPS system. To measure broadband upward and downward longwave radiances and remotely sensed surface temperatures, it is planned to add instruments such as the hemispheric broadband pyranometer (solar) and pyrgeometer (thermal infrared) and the CIMEL/CLIMAT-AV instruments used on the ATR-42. A cooled infrared imaging spectral camera will also be integrated.

MIRA36 is a commercially available METEK Ka-band (36 Ghz) cloud research radar with polarization and Doppler capability to determine vertical velocity in clouds and precipitation. Together with microwave radiometers in the K-, V-, W-, F-, and G-band the MIRA36 is part of HAMP (Mech et al, 2014).

The lidar system WALES is a combined differential absorption and High Spectral Resolution Lidar (HSRL) system developed and built at the Deutsches Zentrum für Luft- und Raumfahrt (Wirth et al, 2009). WALES is capable to nearly simultaneously emit four wavelengths, three online and one offline, in the water vapour absorption band between 935 and 936 nm. The three online wavelengths achieve the necessary sensitivity needed for measurements over the whole range of tropospheric water vapour concentration. The vertical resolution of the raw data is 15 m. In addition to the 935 nm channel, the receiver

Instrument	Brief Description	Reference
BAHAMAS	In situ water vapor, temperature, gust probe winds and aircraft state vector. Up and downward short wave and long wave broadband irradiances (in development)	
HAMP Cloud Radar	Downward staring polarized Doppler 36 Ghz cloud radar	Mech et al (2014)
HAMP Radiometer	Downward staring Microwave Radiometers with 26 channels between 22 and 183 GHz	Mech et al (2014)
WALES	Downward staring water vapor DIAL and backscatter HSRL lidar	Wirth et al (2009)
SMART	Up and downward looking hyper spectral (300-2200 nm) radiance and irradiance measurements	Ehrlich et al (2008)
SpecMACS	Downward looking hyper-spectral (400-2500nm) line imager	Ewald et al (2016)
Thermal Imager	Downward looking (10.8 and 12 μm) two channel line imager (in development)	
Dropsondes	AVAPs System with four channel receiver supporting Vaisala RD94 Sondes (Ten Channel Receiver in development)	

Table 2: Synopsis of HALO instrumentation

is equipped with polarization-sensitive aerosol channels at 532 and 1064 nm, the first one with High Spectral Resolution capabilities using an iodine filter in the detection path (Esselborn et al, 2008). This allows for collocated measurements of humidity, optical depth, clouds and aerosol optical properties.

SpecMACS is an imaging cloud spectrometer developed at LMU (Ewald et al, 2016) consisting of two commercial spectral camera systems in the visible near-infrared (VNIR: 400-1000 nm) and in the shortwave infrared (SWIR: 1000-2500 nm). The nominal spectral resolution is 3 nm and 10 nm for the VNIR and for the SWIR, respectively. SpecMACS produces a spectrally resolved line image. For a flight level of about 10 km, a spatial resolution in the order of 10 m for cloud objects at a distance.

SMART (Spectral Modular Airborne Radiation Measurement System) (Wendisch et al, 2001; Ehrlich et al, 2008) consists of a set of spectral solar radiation sensors including radiances and irradiances (on stabilized platforms). All quantities are obtained for the wavelength range of 0.3–2.2 μm with spectral resolution of 2–16 nm full width of half maximum (FWHM), which is sufficient to analyse the spectral characteristics of spectral absorption bands of ice and liquid water. While the irradiance sensors provide spectral albedo at flight level representative for a specific area, the measurement frequency of 2 Hz and the 2.1° field of view of the radiance sensor allows identifying cloud inhomogeneities (about 200 m footprint for cloud top at 5 km and flight altitude of 10 km).

A similar payload was used during the NARVAL2 campaign and during the NAWDEX campaign of September-October 2016 over the North Atlantic.

Appendix B: Oceanographic instrumentation

The ocean has been historically observed from oceanographic ships and from expendable bathythermograph (XBT) that provides only a very limited spatio-temporal insight of the ocean. Since the early 2000s the advent of the Argo array of autonomous profiling floats has significantly increased the ocean sampling to achieve near-global coverage for the first time over the upper 1800 m. However, these new global observations are still very sparse and do not provide adequate measurements along boundaries of the oceans and within mesoscale eddies. This represents an acute weakness in our present understanding of ocean and atmosphere dynamics and their role in shaping the Earth's climate variability and changes. To confirm, qualify and quantify the role of ocean eddies in the transport of water properties and in air-sea interactions, a number of oceanographic measurements will be necessary.

Ideally, in the year preceding the operational phase of EUREC^{4}A it would be interesting to deploy Argo profiling floats within anticyclonic eddies within the Guiana and North Equatorial currents. By associating these data with satellite observations of the atmosphere (clouds, water vapor, surface winds, etc), it will be possible to follow the joint evolution of eddies and lower atmospheric properties. Then during the operational phase of EUREC^{4}A, it will be appropriate to work with two ships measuring both air-sea fluxes, surface atmospheric properties and vertical profiles of temperature and salinity in the upper 2000 m of the ocean.

Ocean vertical profiles of temperature, salinity, pressure, oxygen and other biogeochemical properties to also assess carbon related quantities will be acquired by a deep-reaching classical CTD rosette, equipped with sampling bottles and Acoustic Doppler Current profilers (ADCP; 150 or 300 kHz; one upward looking and one downward looking). To increase the sampling resolution, it will be very important to implement between CTD stations, at least for temperature, salinity and pressure, a very manageable and easy-to-use vertical profiler such as the Teledyne Underway CTD (UCTD). On both ships, a microstructure vertical profiler would help infer turbulence linked with eddies and air-sea interactions.

The ships should be equipped with an underway Temperature-Salinity measuring system (TSG), and two vessel mounted ADCPs (38 kHz and 75 kHz). They should be also instrumented with standard marine atmospheric observing devices, LIDARs (for vertical profiles of temperature, humidity and wind), as well as instruments that enable to measure local ocean-atmosphere heat and fresh-water fluxes. To complete this set of observations, it would be appropriate to deploy other autonomous observing platforms such as gliders and wave-gliders in the most interesting region identified by the preparing studies, and this sometime before the operational phase of EUREC^{4}A in order to observe the oceanic region and its evolution before, during and after the EUREC^{4}A core field phase.

Acknowledgements The authors gratefully acknowledge Kerry Emanuel for valuable comments and suggestions, and Aurélien Bourdon and the SAFIRE team for useful technical discussions. The paper benefited from stimulating discussions at the International Space Science Institute (ISSI) workshop on "Shallow clouds and water vapor, circulation and climate sensitivity". The EUREC^{4}A project is supported by the European Research Council (ERC), under the European Union's Horizon 2020 research and innovation programme (grant agreement No 694768), by the Max Planck Society and by DFG (Deutsche Forschungsgemeinschaft, German Research Foundation) Priority Program SPP 1294.

References

Albrecht BA, Betts AK, Schubert WH, Cox SK (1979) Model of the thermodynamic structure of the trade-wind boundary layer: Part i. theoretical formulation and sensitivity tests. Journal of the Atmospheric Sciences 36(1):73–89, DOI 10.1175/1520-0469(1979)036<0073:MOTTSO>2.0.CO;2, .

Albrecht BA, Bretherton CS, Johnson D, Scubert WH, Frisch AS (1995) The atlantic stratocumulus transition experiment astex. Bulletin of the American Meteorological Society 76(6):889–904, DOI 10.1175/1520-0477(1995)076<0889:TASTE>2.0.CO;2

Arakawa A, Schubert WH (1974) Interaction of a cumulus cloud ensemble with the large-scale environment, part i. Journal of the Atmospheric Sciences 31(3):674–701, DOI 10.1175/1520-0469(1974)031<0674:IOACCE>2.0.CO;2

Asrar G, Bony S, Boucher O, Busalacchi A, Cazenave A, Dowell M, Flato G, Hegerl G, Kallen E, Nakajima T, Ratier A, Saunders R, Slingo J, Sohn BJ, Schmetz J, Stevens B, Zhang P, Zwiers F (2015) Climate symposium 2014: Findings and recommendations. Bulletin of the American Meteorological Society 96(9):ES145–ES147, DOI 10.1175/BAMS-D-15-00003.1, .

Augstein E, Riehl H, Ostapoff F, Wagner V (1973) Mass and energy transports in an undisturbed atlantic trade-wind flow. Monthly Weather Review 101(2):101–111, DOI 10.1175/1520-0493(1973)101<0101:MAETIA>2.3.CO;2

Augstein E, Schmidt H, Ostapoff F (1974) The vertical structure of the atmospheric planetary boundary layer in undisturbed trade winds over the atlantic ocean. Boundary-Layer Meteorology 6(1):129–150, DOI 10.1007/BF00232480, .

Bony S, Dufresne JL (2005) Marine boundary layer clouds at the heart of tropical cloud feedback uncertainties in climate models. Geophysical Research Letters 32:L20,806, doi: 10.1029/2005GL023,851

Bony S, Dufresne JL, LeTreut H, Morcrette JJ, Senior C (2004) On dynamic and thermodynamic components of cloud changes. Climate Dynamics 22:71–86

Bony S, Stevens B, Frierson DMW, Jakob C, Kageyama M, Pincus R, Shepherd TG, Sherwood SC, Siebesma AP, Sobel AH, Watanabe M, Webb MJ (2015) Clouds, circulation and climate sensitivity. Nature Geoscience 8:261–268, DOI 10.1038/ngeo2398

Borg LA, Bennartz R (2007) Vertical structure of stratiform marine boundary layer clouds and its impact on cloud albedo. Geophysical Research Letters 34(5), DOI 10.1029/2006GL028713, ., l05807

Boucher O, Randall D, Artaxo P, Bretherton C, Feingold G, Forster P, Kerminen VM, Kondo Y, Liao H, Lohmann U, Rasch P, Satheesh S, Sherwood S, Stevens B, Zhang X (2013) Clouds and Aerosols, Cambridge University Press, Cambridge, United Kingdom and New York, NY, USA, book section 7, pp 571–658. DOI 10.1017/CBO9781107415324.016, .

Bretherton CS (2015) Insights into low-latitude cloud feedbacks from high-resolution models. Philosophical Transactions of the Royal Society of London A: Mathematical, Physical and Engineering Sciences 373(2054), DOI 10.1098/rsta.2014.0415

Brient F, Bony S (2012) How may low-cloud radiative properties simulated in the current climate influence low-cloud feedbacks under global warming? Geophysical Research Letters 39(20), DOI 10.1029/2012GL053265, ., l20807

Brient F, Bony S (2013) Interpretation of the positive low-cloud feedback predicted by a climate model under global warming. Climate Dynamics 40(9):2415–2431, DOI 10.1007/s00382-011-1279-7, .

Brient F, Schneider T, Tan Z, Bony S, Qu X, Hall A (2016) Shallowness of tropical low clouds as a predictor of climate models' response to warming. Climate Dynamics 47(1):433–449, DOI 10.1007/s00382-015-2846-0, .

Brogniez G, Pietras C, Legrand M, Dubuisson P, Haeffelin M (2003) A high-accuracy multiwavelength radiometer for in situ measurements in the thermal infrared. part ii: Behavior in field experiments. Journal of Atmospheric and Oceanic Technology 20(7):1023–1033, DOI 10.1175/1520-0426(2003)20<1023:AHMRFI>2.0.CO;2

Bruneau D, Pelon J (2003) Simultaneous measurements of particle backscattering and extinction coefficients and wind velocity by lidar with a mach–zehnder interferometer: principle of operation and performance assessment. Appl Opt 42(6):1101–1114, DOI 10.1364/AO.42.001101, .

Bruneau D, Pelon J, Blouzon F, Spatazza J, Genau P, Buchholtz G, Amarouche N, Abchiche A, Aouji O (2015) 355-nm high spectral resolution airborne lidar lng: system description and first results. Appl Opt 54(29):8776–8785, DOI 10.1364/AO.54.008776, .

Byrne D, Papritz L, Frenger I, MÃ$\frac{1}{4}$nnich M, Gruber N (2015) Atmospheric response to mesoscale sea surface temperature anomalies: Assessment of mechanisms and coupling strength in a high-resolution coupled model over the south atlantic. Journal of the Atmospheric Sciences 72(5):1872–1890, DOI 10.1175/JAS-D-14-0195.1, .

Chazette P, Marnas F, Totems J, Shang X (2014) Comparison of iasi water vapor retrieval with h_2o-raman lidar in the framework of the mediterranean hymex and charmex programs. Atmospheric Chemistry and Physics 14(18):9583–9596, DOI 10.5194/acp-14-9583-2014, .

Chelton DB, Schlax MG, Freilich MH, Milliff RF (2004) Satellite measurements reveal persistent small-scale features in ocean winds. Science 303(5660):978–983, DOI 10.1126/science.1091901, ., .

Ciesielski PE, Schubert WH, Johnson RH (1999) Large-scale heat and moisture budgets over the astex region. Journal of the Atmospheric Sciences 56(18):3241–3261, DOI 10.1175/1520-0469(1999)056<3241:LSHAMB>2.0.CO;2

Cornet C, Labonnote L, Szczap F (2010) Three-dimensional polarized Monte Carlo atmospheric radiative transfer model (3DMCPOL): 3D effects on polarized visible reflectances of a cirrus cloud. Journal of Quantitative Spectroscopy and Radiative Transfer 111(1):174 – 186, DOI http://dx.doi.org/10.1016/j.jqsrt.2009.06.013, .

Dal Gesso S, Siebesma AP, de Roode SR (2015) Evaluation of low-cloud climate feedback through single-column model equilibrium states. Quarterly Journal of the Royal Meteorological Society 141(688):819–832, DOI 10.1002/qj.2398, .

Delanoë J, Protat A, Jourdan O, Pelon J, Papazzoni M, Dupuy R, Gayet JF, Jouan C (2013) Comparison of airborne in situ, airborne radar–lidar, and spaceborne radar–lidar retrievals of polar ice cloud properties sampled during the polarcat campaign. Journal of Atmospheric and Oceanic Technology 30(1):57–73, DOI 10.1175/JTECH-D-11-00200.1

Delanoë J, Protat A, Vinson JP, Brett W, Caudoux C, Bertrand F, du Chatelet JP, Hallali R, Barthes L, Haeffelin M, Dupont JC (2016) Basta: A 95-ghz fmcw doppler radar for cloud and fog studies. Journal of Atmospheric and Oceanic Technology 33(5):1023–1038, DOI 10.1175/JTECH-D-15-0104.1, .

Ehrlich A, Bierwirth E, Wendisch M, Gayet JF, Mioche G, Lampert A, Heintzenberg J (2008) Cloud phase identification of arctic boundary-layer clouds from airborne spectral reflection measurements: test of three approaches. Atmospheric Chemistry and Physics 8(24):7493–7505, DOI 10.5194/acp-8-7493-2008, .

Emanuel KA (1989) The finite-amplitude nature of tropical cyclogenesis. Journal of the Atmospheric Sciences 46(22):3431–3456, DOI 10.1175/1520-0469(1989)046<3431:TFANOT>2.0.CO;2

Esselborn M, Wirth M, Fix A, Tesche M, Ehret G (2008) Airborne high spectral resolution lidar for measuring aerosol extinction and backscatter coefficients. Appl Opt 47(3):346–358, DOI 10.1364/AO.47.000346, .

Ewald F, Kölling T, Baumgartner A, Zinner T, Mayer B (2016) Design and characterization of specMACS, a multipurpose hyperspectral cloud and sky imager. Atmospheric Measurement Techniques 9(5):2015–2042, DOI 10.5194/amt-9-2015-2016, .

Ferreira D, Frankignoul C (2008) Transient atmospheric response to interactive sst anomalies. Journal of Climate 21(3):576–583, DOI 10.1175/2007JCLI1704.1, .

Frenger I, Gruber N, Knutti R, Münnich M (2013) Imprint of southern ocean eddies on winds, clouds and rainfall. Nature Geoscience 6(8):608–612

Gettelman A, Kay JE, Shell KM (2012) The evolution of climate sensitivity and climate feedbacks in the community atmosphere model. Journal of Climate 25(5):1453–1469, DOI 10.1175/JCLI-D-11-00197.1, .

Ghate VP, Miller MA, DiPretore L (2011) Vertical velocity structure of marine boundary layer trade wind cumulus clouds. Journal of Geophysical Research: Atmospheres 116(D16), DOI 10.1029/2010JD015344, ., d16206

Ghate VP, Miller MA, Zhu P (2016) Differences between nonprecipitating tropical and trade wind marine shallow cumuli. Monthly Weather Review 144(2):681–701, DOI 10.1175/MWR-D-15-0110.1, .

Gille ST, Llewellyn Smith SG, Lee SM (2003) Measuring the sea breeze from quikscat scatterometry. Geophysical Research Letters 30(3):n/a–n/a, DOI 10.1029/2002GL016230, ., 1114

Holland JZ (1970) Preliminary report on the bomex sea-air interaction program. Bulletin of the American Meteorological Society 51(9):809–820, DOI 10.1175/1520-0477(1970)051<0809:PROTBS>2.0.CO;2, .

Holland JZ, Rasmusson EM (1973) Measurements of the atmospheric mass, energy, and momentum budgets over a 500-kilometer square of tropical ocean. Monthly Weather Review 101(1):44–55, DOI 10.1175/1520-0493(1973)101<0044:MOTAME>2.3.CO;2, .

Horváth A, Gentemann C (2007) Cloud-fraction-dependent bias in satellite liquid water path retrievals of shallow, non-precipitating marine clouds. Geophysical Research Letters 34(22), DOI 10.1029/2007GL030625, ., l22806

Illingworth AJ, Barker HW, Beljaars A, Ceccaldi M, Chepfer H, Clerbaux N, Cole J, Delanoë J, Domenech C, Donovan DP, Fukuda S, Hirakata M, Hogan RJ, Huenerbein A, Kollias P, Kubota T, Nakajima T, Nakajima TY, Nishizawa T, Ohno Y, Okamoto H, Oki R, Sato K, Satoh M, Shephard MW, Velàzquez-Blàzquez A, Wandinger U, Wehr T, van Zadelhoff GJ (2015) The earthcare satellite: The next step forward in global measurements of clouds, aerosols, precipitation, and radiation. Bulletin of the American Meteorological Society 96(8):1311–1332, DOI 10.1175/BAMS-D-12-00227.1

Karlsson J, Svensson G, Rodhe H (2008) Cloud radiative forcing of subtropical low level clouds in global models. Climate Dynamics 30(7):779–788, DOI 10.1007/s00382-007-0322-1, .

Kollias P, Albrecht B (2010) Vertical velocity statistics in fair-weather cumuli at the arm twp nauru climate research facility. Journal of Climate 23(24):6590–6604, DOI 10.1175/2010JCLI3449.1, .

Lamer K, Kollias P, Nuijens L (2015) Observations of the variability of shallow trade wind cumulus cloudiness and mass flux. Journal of Geophysical Research: Atmospheres 120(12):6161–6178, DOI 10.1002/2014JD022950, ., 2014JD022950

Laxenaire R, Sabrina S, Blanke B, Chaigneau A, Pegliasco C (in preparation) A new insight on the indo-atlantic exchange achieved by indian ocean eddies assessed by satellite altimetry. Geophysical Research Letters

LeMone MA, Pennell WT (1976) The relationship of trade wind cumulus distribution to subcloud layer fluxes and structure. Monthly Weather Review 104(5):524–539, DOI 10.1175/1520-0493(1976)104<0524:TROTWC>2.0.CO;2, .

Lenschow DH, Savic-Jovcic V, Stevens B (2007) Divergence and vorticity from aircraft air motion measurements. Journal of Atmospheric and Oceanic

Technology 24(12):2062–2072, DOI 10.1175/2007JTECHA940.1, .
Matheou G, Chung D, Nuijens L, Stevens B, Teixeira J (2011) On the fidelity of large-eddy simulation of shallow precipitating cumulus convection. Monthly Weather Review 139(9):2918–2939, DOI 10.1175/2011MWR3599.1, .
Mayer, B (2009) Radiative transfer in the cloudy atmosphere. EPJ Web of Conferences 1:75–99, DOI 10.1140/epjconf/e2009-00912-1, .
McWilliams JC (2016) Submesoscale currents in the ocean. Proceedings of the Royal Society of London A: Mathematical, Physical and Engineering Sciences 472(2189), DOI 10.1098/rspa.2016.0117, ., .
Mech M, Orlandi E, Crewell S, Ament F, Hirsch L, Hagen M, Peters G, Stevens B (2014) Hamp – the microwave package on the high altitude and long range research aircraft (halo). Atmospheric Measurement Techniques 7(12):4539–4553, DOI 10.5194/amt-7-4539-2014, .
Medeiros B, Nuijens L (2016) Clouds at barbados are representative of clouds across the trade wind regions in observations and climate models. Proceedings of the National Academy of Sciences 113(22):E3062–E3070, DOI 10.1073/pnas.1521494113, .
Medeiros B, Stevens B, Held I, Zhao M, Williamson DL, Olson J, Bretherton C (2008) Aquaplanets, climate sensitivity, and low clouds. Journal of Climate 21:4974–4991
Medeiros B, Stevens B, Bony S (2015) Using aquaplanets to understand the robust responses of comprehensive climate models to forcing. Climate Dynamics 44(7):1957–1977, DOI 10.1007/s00382-014-2138-0, .
Muller CJ, Held IM (2012) Detailed Investigation of the Self-Aggregation of Convection in Cloud-Resolving Simulations. Journal of Atmospheric Sciences 69:2551–2565, DOI 10.1175/JAS-D-11-0257.1
Nam C, Bony S, Dufresne JL, Chepfer H (2012) The 'too few, too bright' tropical low-cloud problem in cmip5 models. Geophysical Research Letters 39(21), DOI 10.1029/2012GL053421, ., l21801
Neggers R, Stevens B, Neelin JD (2006) A simple equilibrium model for shallow-cumulus-topped mixed layers. Theoretical and Computational Fluid Dynamics 20(5):305–322, DOI 10.1007/s00162-006-0030-1, .
Neggers RAJ (2015) Exploring bin-macrophysics models for moist convective transport and clouds. Journal of Advances in Modeling Earth Systems 7(4):2079–2104, DOI 10.1002/2015MS000502, .
Nitta T, Esbensen S (1974a) Diurnal variations in the western atlantic trades during the bomex. Journal of the Meteorological Society of Japan Ser II 52(2):254–257
Nitta T, Esbensen S (1974b) Heat and moisture budget analyses using bomex data. Monthly Weather Review 102(1):17–28, DOI 10.1175/1520-0493(1974)102<0017:HAMBAU>2.0.CO;2, .
Nitta T, Esbensen S (1974b) Diurnal variations in the western atlantic trades during the bomex. Journal of the Meteorological Society of Japan Ser II 52(2):254–257
Norris JR (1998) Low cloud type over the ocean from surface observations. Part II: geographical and seasonal variations. Journal of Climate 11:383–

403
Nuijens L, Stevens B, Siebesma AP (2009) The environment of precipitating shallow cumulus convection. Journal of the Atmospheric Sciences 66(7):1962–1979, DOI 10.1175/2008JAS2841.1

Nuijens L, Serikov I, Hirsch L, Lonitz K, Stevens B (2014) The distribution and variability of low-level cloud in the north atlantic trades. Quarterly Journal of the Royal Meteorological Society 140(684):2364–2374, DOI 10.1002/qj.2307, .

Nuijens L, Medeiros B, Sandu I, Ahlgrimm M (2015) The behavior of tradewind cloudiness in observations and models: The major cloud components and their variability. Journal of Advances in Modeling Earth Systems 7(2):600–616, DOI 10.1002/2014MS000390, .

Oue M, Kollias P, North KW, Tatarevic A, Endo S, Vogelmann AM, Gustafson WI (2016) Estimation of cloud fraction profile in shallow convection using a scanning cloud radar. Geophysical Research Letters 43(20):10,998–11,006, DOI 10.1002/2016GL070776, ., 2016GL070776

Polichtchouk I, Shepherd TG (2016) Zonal-mean circulation response to reduced air-sea momentum roughness. Quarterly Journal of the Royal Meteorological Society 142(700):2611–2622, DOI 10.1002/qj.2850, .

Rauber RM, III HTO, Girolamo LD, Göke S, Snodgrass E, Stevens B, Knight C, Jensen JB, Lenschow DH, Rilling RA, Rogers DC, Stith JL, Albrecht BA, Zuidema P, Blyth AM, Fairall CW, Brewer WA, Tucker S, Lasher-Trapp SG, Mayol-Bracero OL, Vali G, Geerts B, Anderson JR, Baker BA, Lawson RP, Bandy AR, Thornton DC, Burnet E, Brenguier JL, Gomes L, Brown PRA, Chuang P, Cotton WR, Gerber H, Heikes BG, Hudson JG, Kollias P, Krueger SK, Nuijens L, O'Sullivan DW, Siebesma AP, Twohy CH (2007) Rain in shallow cumulus over the ocean: The rico campaign. Bulletin of the American Meteorological Society 88(12):1912–1928, DOI 10.1175/BAMS-88-12-1912, .

Raymond DJ (1995) Regulation of moist convection over the west pacific warm pool. Journal of the Atmospheric Sciences 52(22):3945–3959, DOI 10.1175/1520-0469(1995)052<3945:ROMCOT>2.0.CO;2

Rieck M, Nuijens L, Stevens B (2012) Marine Boundary Layer Cloud Feedbacks in a Constant Relative Humidity Atmosphere. Journal of Atmospheric Sciences 69:2538–2550, DOI 10.1175/JAS-D-11-0203.1

Roca R, Brogniez H, Chambon P, Chomette O, Cloché S, Gosset ME, Mahfouf JF, Raberanto P, Viltard N (2015) The Megha-Tropiques mission: a review after three years in orbit. Frontiers in Earth Science 3:17, DOI 10.3389/feart.2015.00017, .

Rodts SMA, Duynkerke PG, Jonker HJJ (2003) Size distributions and dynamical properties of shallow cumulus clouds from aircraft observations and satellite data. Journal of the Atmospheric Sciences 60(16):1895–1912, DOI 10.1175/1520-0469(2003)060<1895:SDADPO>2.0.CO;2, .

Ruppert JH (2016) Diurnal timescale feedbacks in the tropical cumulus regime. Journal of Advances in Modeling Earth Systems 8(3):1483–1500, DOI 10.1002/2016MS000713, .

Ruppert JH, Johnson RH (2015) Diurnally modulated cumulus moistening in the preonset stage of the madden-julian oscillation during dynamo. Journal of the Atmospheric Sciences 72(4):1622–1647, DOI 10.1175/JAS-D-14-0218.1, .

Ruppert JH, Johnson RH (2016) On the cumulus diurnal cycle over the tropical warm pool. Journal of Advances in Modeling Earth Systems 8(2):669–690, DOI 10.1002/2015MS000610, .

Schlemmer L, Bechtold P, Sandu I, Ahlgrimm M (submitted) Uncertainties related to the representation of momentum transport in shallow convection. Journal of Advances in Modeling Earth Systems

Seifert A, Heus T (2013) Large-eddy simulation of organized precipitating trade wind cumulus clouds. Atmospheric Chemistry and Physics 13(11):5631–5645, DOI 10.5194/acp-13-5631-2013, .

Sherwood SC, Bony S, Dufresne JL (2014) Spread in model climate sensitivity traced to atmospheric convective mixing. Nature 505:37–42, DOI 10.1038/nature12829

Siebesma AP, Cuijpers JWM (1995) Evaluation of parametric assumptions for shallow cumulus convection. Journal of the Atmospheric Sciences 52(6):650–666, DOI 10.1175/1520-0469(1995)052<0650:EOPAFS>2.0.CO;2, .

Siebesma AP, Bretherton CS, Brown A, Chlond A, Cuxart J, Duynkerke PG, Jiang H, Khairoutdinov M, Lewellen D, Moeng CH, Sanchez E, Stevens B, Stevens DE (2003) A large eddy simulation intercomparison study of shallow cumulus convection. Journal of the Atmospheric Sciences 60(10):1201–1219, DOI 10.1175/1520-0469(2003)60<1201:ALESIS>2.0.CO;2

Simpson IR, Shaw TA, Seager R (2014) A diagnosis of the seasonally and longitudinally varying midlatitude circulation response to global warming. Journal of the Atmospheric Sciences 71(7):2489–2515, DOI 10.1175/JAS-D-13-0325.1

Stevens B (2006) Bulk boundary-layer concepts for simplified models of tropical dynamics. Theoretical and Computational Fluid Dynamics 20(5):279–304, DOI 10.1007/s00162-006-0032-z, .

Stevens B, Ackerman AS, Albrecht BA, Brown AR, Chlond A, Cuxart J, Duynkerke PG, Lewellen DC, Macvean MK, Neggers RAJ, SÃ¡nchez E, Siebesma AP, Stevens DE (2001) Simulations of trade wind cumuli under a strong inversion. Journal of the Atmospheric Sciences 58(14):1870–1891, DOI 10.1175/1520-0469(2001)058<1870:SOTWCU>2.0.CO;2, .

Stevens B, Farrell D, Hirsch L, Jansen F, Nuijens L, Serikov I, Brügmann B, Forde M, Linne H, Lonitz K, Prospero JM (2016) The barbados cloud observatory: Anchoring investigations of clouds and circulation on the edge of the itcz. Bulletin of the American Meteorological Society 97(5):787–801, DOI 10.1175/BAMS-D-14-00247.1, .

Stubenrauch CJ, Rossow WB, Kinne S, Ackerman S, Cesana G, Chepfer H, Girolamo LD, Getzewich B, Guignard A, Heidinger A, Maddux BC, Menzel WP, Minnis P, Pearl C, Platnick S, Poulsen C, Riedi J, Sun-Mack S, Walther A, Winker D, Zeng S, Zhao G (2013) Assessment of global cloud datasets from satellites: Project and database initiated by the gewex radiation panel. Bulletin of the American Meteorological Society 94(7):1031–1049, DOI 10.1175/BAMS-D-12-00117.1, .

Szczap F, Cornet C, Alkasem A, Gour Y, Labonnote L, Jourdan O (2013) A 3D Polarized Monte Carlo LIDAR System Simulator for Studying Effects of Cirrus Inhomogeneities on CALIOP/CALIPSO Measurements. IRS2012 Proceedings

Thayer-Calder K, Randall D (2015) A numerical investigation of boundary layer quasi-equilibrium. Geophysical Research Letters 42(2):550–556, DOI 10.1002/2014GL062649, ., 2014GL062649

Tomassini L, Voigt A, Stevens B (2015) On the connection between tropical circulation, convective mixing, and climate sensitivity. Quarterly Journal of the Royal Meteorological Society 141(689):1404–1416, DOI 10.1002/qj.2450, .

vanZanten MC, Stevens B, Nuijens L, Siebesma AP, Ackerman AS, Burnet F, Cheng A, Couvreux F, Jiang H, Khairoutdinov M, Kogan Y, Lewellen DC, Mechem D, Nakamura K, Noda A, Shipway BJ, Slawinska J, Wang S, Wyszogrodzki A (2011) Controls on precipitation and cloudiness in simulations of trade-wind cumulus as observed during rico. Journal of Advances in Modeling Earth Systems 3(2), DOI 10.1029/2011MS000056, ., m06001

Vial J, Dufresne JL, Bony S (2013) On the interpretation of inter-model spread in cmip5 climate sensitivity estimates. Climate Dynamics 41(11):3339–3362, DOI 10.1007/s00382-013-1725-9, .

Vial J, Bony S, Dufresne JL, Roehrig R (2016) Coupling between lower-tropospheric convective mixing and low-level clouds: Physical mechanisms and dependence on convection scheme. Journal of Advances in Modeling Earth Systems DOI 10.1002/2016MS000740, .

Vogel R, Nuijens L, Stevens B (2016) The role of precipitation and spatial organization in the response of trade-wind clouds to warming. Journal of Advances in Modeling Earth Systems 8(2):843–862, DOI 10.1002/2015MS000568, .

Wang J, Carton JA (2003) Modeling climate variability in the tropical atlantic atmosphere. Journal of Climate 16(23):3858–3876, DOI 10.1175/1520-0442(2003)016<3858:MCVITT>2.0.CO;2

Wang JJ, Young K, Hock T, Lauritsen D, Behringer D, Black M, Black PG, Franklin J, Halverson J, Molinari J, Nguyen L, Reale T, Smith J, Sun B, Wang Q, Zhang JA (2015) A long-term, high-quality, high-vertical-resolution gps dropsonde dataset for hurricane and other studies. Bulletin of the American Meteorological Society 96(6):961–973, DOI 10.1175/BAMS-D-13-00203.1, .

Webb M, Senior C, Sexton D, Ingram W, Williams K, Ringer M, McAvaney B, Colman R, Soden B, Gudgel R, et al (2006) On the contribution of local feedback mechanisms to the range of climate sensitivity in two gcm ensembles. Climate Dynamics 27(1):17–38

Webb MJ, Lock AP, Bretherton CS, Bony S, Cole JNS, Idelkadi A, Kang SM, Koshiro T, Kawai H, Ogura T, Roehrig R, Shin Y, Mauritsen T, Sherwood SC, Vial J, Watanabe M, Woelfle MD, Zhao M (2015) The impact of parametrized convection on cloud feedback. Philosophical Transactions of the Royal Society of London A: Mathematical, Physical and Engineering Sciences 373(2054), DOI 10.1098/rsta.2014.0414, .

Wendisch M, Brenguier JL (2013) Wiley-VCH Verlag GmbH & Co. KGaA, Weinheim, Germany, p 655 pp. DOI 10.1002/9783527653218

Wendisch M, Müller D, Schell D, Heintzenberg J (2001) An airborne spectral albedometer with active horizontal stabilization. Journal of Atmospheric and Oceanic Technology 18(11):1856–1866, DOI 10.1175/1520-0426(2001)018<1856:AASAWA>2.0.CO;2

Wendisch M, Pöschl U, Andreae MO, Machado LAT, Albrecht R, Schlager H, Rosenfeld D, Martin ST, Abdelmonem A, Afchine A, Araùjo AC, Artaxo P, Aufmhoff H, Barbosa HMJ, Borrmann S, Braga R, Buchholz B, Cecchini MA, Costa A, Curtius J, Dollner M, Dorf M, Dreiling V, Ebert V, Ehrlich A, Ewald F, Fisch G, Fix A, Frank F, Fütterer D, Heckl C, Heidelberg F, Hüneke T, Jäkel E, Järvinen E, Jurkat T, Kanter S, Kästner U, Kenntner M, Kesselmeier J, Klimach T, Knecht M, Kohl R, Kölling T, Krämer M, Krüger M, Krisna TC, Lavric JV, Longo K, Mahnke C, Manzi AO, Mayer B, Mertes S, Minikin A, Molleker S, MÃ¼nch S, Nillius B, Pfeilsticker K, Pöhlker C, Roiger A, Rose D, Rosenow D, Sauer D, Schnaiter M, Schneider J, Schulz C, de Souza RAF, Spanu A, Stock P, Vila D, Voigt C, Walser A, Walter D, Weigel R, Weinzierl B, Werner F, Yamasoe MA, Ziereis H, Zinner T, Zöger M (2016) Acridicon-chuva campaign: Studying tropical deep convective clouds and precipitation over amazonia using the new german research aircraft halo. Bulletin of the American Meteorological Society 97(10):1885–1908, DOI 10.1175/BAMS-D-14-00255.1

Wentz FJ, Spencer RW (1998) Ssm/i rain retrievals within a unified all-weather ocean algorithm. Journal of the Atmospheric Sciences 55(9):1613–1627, DOI 10.1175/1520-0469(1998)055<1613:SIRRWA>2.0.CO;2

Winker DM, Pelon J, McCormick MP (2003) The CALIPSO mission: Spaceborne lidar for observation of aerosols and clouds. Proc SPIE 4893:1–11

Wirth M, Fix A, Mahnke P, Schwarzer H, Schrandt F, Ehret G (2009) The airborne multi-wavelength water vapor differential absorption lidar wales: system design and performance. Applied Physics B 96(1):201, DOI 10.1007/s00340-009-3365-7, .

Wood R, Köhler M, Bennartz R, O'Dell C (2009) The diurnal cycle of surface divergence over the global oceans. Quarterly Journal of the Royal Meteorological Society 135(643):1484–1493, DOI 10.1002/qj.451, .

Yanai M, Esbensen S, Chu JH (1973) Determination of bulk properties of tropical cloud clusters from large-scale heat and moisture budgets. Journal of the Atmospheric Sciences 30(4):611–627, DOI 10.1175/1520-0469(1973)030¡0611:DOBPOT¿2.0.CO;2, .

Zhang M, Bretherton C (2008) Mechanisms of low cloud-climate feedback in idealized single-column simulations with the community atmospheric model, version 3 (cam3). Journal of Climate 21(18):4859–4878, DOI 10.1175/2008JCLI2237.1, .

Zhang M, Bretherton CS, Blossey PN, Austin PH, Bacmeister JT, Bony S, Brient F, Cheedela SK, Cheng A, Genio AD, Roode SR, Endo S, Franklin CN, Golaz JC, Hannay C, Heus T, Isotta FA, Dufresne JL, Kang IS, Kawai H, Köhler M, Larson VE, Liu Y, Lock AP, Lohmann U, Khairoutdinov MF, Molod AM, Neggers RAJ, Rasch P, Sandu I, Senkbeil R, Siebesma AP, Siegenthaler-Le Drian C, Stevens B, Suarez MJ, Xu KM, Salzen K, Webb MJ, Wolf A, Zhao M (2013) CGILS: Results from the first phase of an international project to understand the physical mechanisms of low cloud feedbacks in single column models. Journal of Advances in Modeling Earth Systems 5:826–842, DOI 10.1002/2013MS000246

Zhang Z, Zhang Y, Wang W, Huang RX (2013) Universal structure of mesoscale eddies in the ocean. Geophysical Research Letters 40(14):3677–3681, DOI 10.1002/grl.50736, .

Zhao G, Di Girolamo L (2007) Statistics on the macrophysical properties of trade wind cumuli over the tropical western atlantic. Journal of Geophysical Research: Atmospheres 112(D10):n/a–n/a, DOI 10.1029/2006JD007371, ., d10204

Zinner T, Mayer B, Schröder M (2006) Determination of three-dimensional cloud structures from high-resolution radiance data. Journal of Geophysical Research: Atmospheres 111(D8), DOI 10.1029/2005JD006062, ., d08204